Determining the strength of undetectable particle-hole configurations by complete spectroscopy of negative parity states in ^{208}Pb

A. Heusler*
Gustav-Kirchhoff-Strasse 7/1, D-69120 Heidelberg, Germany

T. Faestermann
Physik Department E12, Techn. Universität München, D-85748 Garching, Germany

R. Hertenberger and H.-F. Wirth
Fakultät für Physik, Ludwig-Maximilians-Universität München, D-85748 Garching, Germany

P. von Brentano
Institut für Kernphysik, Universität zu Köln, D-50937 Köln, Germany
(Received 9 September 2013; published 28 February 2014)

In the doubly magic nucleus ^{208}Pb, many states contain fractions of particle-hole configurations whose strength can be determined from experiment. However, some configurations are not excited in a directly detectable way. Their strengths can be determined by observing an ensemble of states which consists entirely of an equivalent set of configurations with a given spin and parity among which only one or two configurations are not detected. Examples for spins 2^-–5^- are evaluated. Excitation energies of states in ^{208}Pb are determined with a precision down to 100 eV by experiments on the ^{208}Pb(p,p') and ^{207}Pb(d,p) reactions with the Q3D magnetic spectrograph (Maier-Leibnitz-Laboratorium, Garching, Germany). Six doublets with distances between the states of less than 2 keV are resolved. 72 negative parity states below $E_x = 6.1$ MeV are identified. They correspond to 70 states predicted by the schematic shell model without residual interaction below $E_x = 6361$ keV. The 1^- and 3^- yrast states appear in addition. Six new spins are assigned to negative parity states, three new spins to positive parity states, and two spins suggested by the Nuclear Data Sheets are verified. The state at $E_x = 4953$ keV is identified as the 3^+ member of the configuration $g_{9/2}i_{13/2}$. Among about hundred states, the configuration mixing for unnatural parity is shown to be less than for natural parity.

DOI: 10.1103/PhysRevC.89.024322 PACS number(s): 21.60.Cs, 21.10.Hw, 24.30.Gd, 27.80.+w

I. INTRODUCTION

Inelastic proton scattering on ^{208}Pb via isobaric analog resonances (IARs) in ^{209}Bi excites neutron particle-hole configurations in states of ^{208}Pb [1–9]. Spectroscopic information about proton particle-hole configurations can be obtained for the configurations with an $h_{9/2}$ particle [10–12]; other proton particle-hole configurations are undetectable.

The schematic shell model without residual interaction (SSM) [13] describes about a hundred states below $E_x = 6.1$ MeV quite well. Not all predicted states are identified, however. The Nuclear Data Sheets (NDS2007) [14] list nearly 150 levels with excitation energy below $E_x = 6.1$ MeV and firmly assigned spin and parity or suggested assignments. Several levels were recently associated with newly identified states; for a lot of states new spin and parity have been assigned and components of the configuration mixing have been determined [13,15–25].

A set of states with the same spin and parity is called an ensemble. Some ensembles of states (especially with negative parity) are well described by a unitary transformation of a group of SSM configurations. For such an ensemble the amplitudes of an undetectable configuration can be deduced if all other amplitudes are sufficiently well known. An example has been given by the determination of the mixing between the neutron particle-hole configuration $i_{11/2}p_{3/2}$ and the proton particle-hole configuration $f_{7/2}d_{3/2}$ in the 4^- states at $E_x = 5239, 5276$ keV; a mixing ratio of 9:1 has been determined [15]. Less than a few percent strength of other configurations contributes to either state.

The strength of the proton particle-hole configurations $f_{7/2}s_{1/2}$, $f_{7/2}d_{3/2}$ can be determined only indirectly: No target of ^{209}Bi in the $f_{7/2}$ state can be prepared, hence corresponding proton transfer reactions cannot be studied. Nevertheless, by determining the strength of all other neighboring configurations, the main components of the two configurations $f_{7/2}s_{1/2}$, $f_{7/2}d_{3/2}$ are almost completely deduced. The strengths of some other particle-hole configurations are difficult to determine because of more technical reasons; these configurations are in fact also undetectable.

The experimental work relies on the high precision and the fast performance of the Q3D magnetic spectrograph at the Maier-Leibnitz-Laboratorium (MLL) at Garching, Germany [26–28]. A resolution of 1.5 keV HWHM (half-width at half-maximum) on the low-energy side [13] and peak-to-valley ratios up to 10 000:1 are achieved; the high luminosity allows us to obtain 100 counts in half an hour for a peak of 1 μbr/sr. Upper limits of cross sections as low as 0.5 μb/sr are reliably obtained. Excitation energies up to 8 MeV are determined with

*Corresponding author: A.Heusler@mpi-hd.mpg.de

a precision down to 100 eV (if the statistics are sufficiently high) because of the high linearity of the Q3D magnetic spectrograph.

The work of NDS2007 provides the basis as well for the identification of states as for spin, parity, and configuration assignments—both firm assignments and a suggested range. Recent work identified some new states, reassigned or newly assigned spin and parity of many states in ^{208}Pb, and revealed both dominant configurations and weak admixtures [13,15–20]. Several doublets with distances down to 400 eV and even vanishing distances are disentangled.

In this paper, six more doublets and a few weakly excited states are discussed. Preferentially, the configuration mixing in negative parity states is discussed while positive parity states are discussed in a minimal manner. No effort is made to discuss all states with the goal to eliminate spurious states.

Together with NDS2007 and other recent publications, all 70 negative parity states predicted by the schematic shell model below $E_x^{\rm SSM} = 6361$ keV are identified [25]. Most unnatural parity states are described by one or two configurations with less than 10% strength in other configurations; for natural parity states up to four configurations are mostly needed to gain more than 90% of the total strength. The 1^- yrast and 3^- yrast states show up in addition to this prediction; neither state has a dominant configuration, and the strengths of all detectable configurations are below a few percent.

The paper has three major sections, Secs. II, III, and IV. In Sec. II A the space of the SSM configurations is explained. In Sec. II B the unitarity conditions for the transformation matrices between the SSM configurations and the physical states are discussed. In Sec. II C we discuss the methods to determine the configuration mixing, in Sec. II D methods of spin and parity assignment by particle spectroscopy, and in Sec. II E methods to determine configuration strengths.

In Sec. III A the problems with resolution, peak shape, and doublets are discussed. In Sec. III B new spectra for ^{208}Pb(p,p') are explained. Appendix A lists spectra for the ^{208}Pb(p,p') and ^{207}Pb(d,p) reactions shown in previous papers. In Sec. III C poorly resolved 1-keV and 2-keV doublets and in Sec. III D states weakly excited by the ^{208}Pb(p,p') and the ^{207}Pb(d,p) reactions are discussed. Finally, in Sec. III E data from other experiments are mentioned.

In Sec. IV A confirmed spin assignments for negative parity states and in Sec. IV B the two major fractions of configurations in each state are discussed. In Sec. IV C new spin and parity assignments and confirmed suggestions are presented. In Sec. IV D the location of the dominant particle-hole configuration strength and in Sec. IV E the difference in the mixing among configurations with unnatural and natural parity are discussed. Finally, in Sec. IV F the centroid energies and the influence of the Coulomb force on the proton configurations are discussed.

II. EXPERIMENTAL DETERMINATION OF PARTICLE-HOLE CONFIGURATION STRENGTHS

A. The schematic shell model

The schematic shell model without residual interaction (SSM) describes most states in ^{208}Pb by the coupling of a single particle in the neighboring nuclei ^{209}Pb, ^{209}Bi and of a single hole in ^{207}Pb, ^{207}Tl to neutron and proton particle-hole configurations, respectively [13]. The excitation energies are predicted by adding up the excitation energies in the nuclei with one particle and one hole, their mass differences, and the correction for the change of the Coulomb energy with atomic weight.

(In this paper, a state in ^{208}Pb is denoted by an energy label $\tilde{E}_x$ chosen to reflect the excitation energy given by NDS2007 in a unique manner, spin I and parity π; e.g., 4712 4^-.) In reality, each state is described by a superposition of several configurations where a particle in orbit LJ couples to a hole in orbit lj,

$$|\tilde{E}_x, I^\pi\rangle = \sum_{LJ} \sum_{lj} c_{LJ,lj}^{\tilde{E}_x I^\pi} |(LJ \otimes lj)I\rangle. \quad (1)$$

(Due to the time-reversal invariance of the Hamiltonian, the amplitudes $c_{LJ,lj}^{\tilde{E}_x I^\pi}$ are real [29].)

We arrange the states and the configurations by their excitation energy (Table I) and thus define order numbers M,m for each spin and parity I^π, respectively,

$$\begin{aligned} |\tilde{E}_x, I^\pi\rangle &\equiv |I_M^\pi\rangle, \\ |(LJ \otimes lj)I\rangle &\equiv |I_m^\pi\rangle. \end{aligned} \quad (2)$$

Synonyms of the amplitude are then defined as

$$c_{M,m}^{I^\pi} \equiv c_{M,LJ\,lj}^{I^\pi} \equiv c_{LJ,lj}^{\tilde{E}_x I^\pi} \quad (3)$$

by either choosing the order number M or the energy label $\tilde{E}_x$ to characterize the state, and either the order number m or the combination of the particle LJ and the hole lj or $LJ\,lj$ to characterize the configuration. Equation (1) can be thus written in a synonymous manner as

$$|I_M^\pi\rangle = \sum_m c_{M,m}^{I^\pi} |I_m^\pi\rangle, \quad (4)$$

$$\text{or} \quad |I_M^\pi\rangle = \sum_{LJ\,lj} c_{M,LJ\,lj}^{I^\pi} |(LJ\,lj)_I\rangle. \quad (5)$$

Mostly a state with order number M has a dominant configuration $LJ\,lj$ of the same order number ($M = m$), but in some cases the order numbers M,m differ. (Especially, the states 1^- and 3^- states below 6.1 MeV following the yrast states mostly have $M = m + 1$.) If the configuration mixing is large then the correspondence between the configuration number m and the dominant configuration $LJ\,lj$ is arbitrary. Yet, for a given spin I^π, each configuration must be assigned as being dominant once only in some state in order to achieve a unique equivalence between configuration number m and dominant configuration $LJ\,lj$ in the state.

For all states, the strengths of only one, two, or three leading configurations among up to sixteen configurations in Eqs. (1), (4), and (5) are considered in this paper. The contribution of a few more configurations is discussed. In some cases, weak admixtures down to 0.1% are decisive for the assignment of spin and parity.

As a complement to Table I, Ref. [21] shows the level scheme for the SSM configurations and the states in ^{208}Pb for each of the spins $2^-, 4^-, 6^-, 7^-, 8^-$ (and also $1^+, 3^+, 5^+, 7^+,$

TABLE I. Multiplets of SSM configurations in ^{208}Pb with negative parity below $E_x^{\mathrm{SSM}} = 6536$ keV. There are two kinds of entries with corresponding headings. In the first line the information for each SSM configuration $LJ\,lj$ with order number m is shown, the next lines show the information for each member of the multiplet $LJ\,lj$ with spin I^π. The centroid energy $\overline{E_x^{\mathrm{cnt}}}$ and the spin weighted sum of the strength $S_{LJ\,lj}$ for each configuration are printed *italic*. For each spin I^π, the centroid energy E_x^{cnt}, order number M, as well as energy label $\tilde{E}_x$ and strength c^2 of one or two states bearing large fraction of the SSM configuration are shown. Strengths are shown by values of 98%, 95%, 90%, 80% with uncertainties of about 1%, 3%, 5%, 10%–30%, respectively; other values have varying uncertainties (Sec. II E). The determination of the dominant configuration strength is discussed on the basis of the given reference; see Sec. IV D. The next leading strengths are discussed in Secs. IV A and IV C. Energy labels of states with new spin and parity assignments are printed boldface; confirmed or verified assignments are printed italic. Energy labels $\tilde{E}_x$ for states with new spin assignments since the publication of NDS2007 are underlined (Sec. IV A 2).

Configuration				All States						
E_x^{SSM} (keV)	$\overline{E_x^{\mathrm{cnt}}}$ [Eq. (19)] (MeV)	LJ lj		m			$S_{LJ,lj}$ [Eq. (10)] ×100			
					1. State				2. State	
	E_x^{cnt} [Eq. (18)] (MeV)		I^π		M	$\tilde{E}_x$	c^2 [Eq. (1)] ×100	Ref.	$\tilde{E}_x$	c^2 [Eq. (1)] ×100
			1^-	[a]	1	4841	[b]	[14]		
			3^-	[a]	1	2615	[b]	[14]		
3431	*3.40*	$g_{9/2}$ $p_{1/2}$					*86*			
	3.49		4^-	1	1	3475	92	[30]	3995	2
	3.33		5^-	1	1	3198	60	[31]	3708	20
3914	*3.91*	$h_{9/2}$ $s_{1/2}$					*86*			
	3.95		4^-	2	2	3947	90	[10]	4262	5
	3.88		5^-	2	3	3961	50	[10]	3708	25
4001	*3.99*	$g_{9/2}$ $f_{5/2}$					*86*			
	4.23		2^-	1	1	4230	95	[29]		
	4.20		3^-	1	3	4255	60	[29]	4051	20
	3.99		4^-	3	3	3995	95	[31]	3947	5
	3.79		5^-	3	2	3708	50	[31]	3961	25
	3.92		6^-	1	1	3920	95	[31]	4383	5
	4.03		7^-	1	1	4037	75	[29]		
4210	*4.19*	$i_{11/2}$ $p_{1/2}$					*84*			
	4.16		5^-	4	5	4180	50	[31]	4125	20
	4.22		6^-	2	2	4206	90	[31]	4383	5
4265	*4.33*	$h_{9/2}$ $d_{3/2}$					*82*			
	4.18		3^-	2	2	4051	40	[29]	4698	10
	4.29		4^-	4	4	4262	60	[10]	4359	30
	4.22		5^-	5	4	4125	35	[10]	4297	40
	4.40		6^-	3	3	4383	80	[10]	4481	15
4329	*4.38*	$g_{9/2}$ $p_{3/2}$					*84*			
	4.51		3^-	3	4	4698	50	[29]	4051	20
	4.35		4^-	5	5	4359	70	[31]	4262	10
	4.20		5^-	6	6	4297	40	[31]	4180	35
	4.47		6^-	4	4	4481	80	[31]	4383	15

TABLE I. (*Continued.*)

E_x^{SSM}	E_x^{cnt}	LJ lj	I^π	m	M	$\tilde{E}_x(1)$	c_1^2	Ref.	$\tilde{E}_x(2)$	c_2^2
4780	*4.78*	$i_{11/2}$ $f_{5/2}$					*92*			
	4.94		3^-	4	5	4937	70	[c]		
	4.71		4^-	6	6	4712	90	[15]		
	4.71		5^-	7	7	4709	90	[15]		
	4.76		6^-	5	5	4762	95	[15]		
	4.68		7^-	2	2	4680	95	[15]		
	4.92		8^-	1	1	4919	98	[15]		
4811	*5.03*	$f_{7/2}$ $s_{1/2}$					*81*			
	5.19		3^-	5	7	**5195**	60[d]	[c]		
	4.91		4^-	7	7	*4911*	90[d]	[c]		
4998	*5.07*[e]	$d_{5/2}$ $p_{1/2}$					*78*[e]			
	5.07[e]		2^-	2	2	5038	60	[20]	5127	30
	5.08[e]		3^-	6	6	4974	50	[20]	5245	30
5108	*5.11*	$i_{11/2}$ $p_{3/2}$					*96*			
	5.27		4^-	8	9	5276	90	[15]	5239	10
	5.07		5^-	8	8	5075	95	[15]		
	5.08		6^-	6	6	5080	95	[15]		
	5.08		7^-	3	3	5085	95	[15]		
5162	*5.21*	$f_{7/2}$ $d_{3/2}$					*73*			
	5.09		2^-	3	3	5127	50[d]	[20]	5038	30[d]
	5.30		3^-	7	8	5245	30[d]	[c]	5347	30[d]
	5.24		4^-	9	8	5239	90[d]	[15]	5276	10[d]
	5.21		5^-	9	9	*5214*	70[d]	[c]		
5463	*5.33*	$s_{1/2}$ $p_{1/2}$					*92*			
	5.32		0^-	1	1	5280	87	[16]	5599	13
	5.34		1^-	1	2	5292	80	[16]	5512	10
5568	*5.53*	$d_{5/2}$ $f_{5/2}$					*76*			
	5.56		0^-	2	2	5599	87	[16]	5280	13
	5.46		1^-	2	3	5512	70	[c]	5292	20
	5.64		2^-	4	5	**5643**	40	[c]	5548	40
	5.46		3^-	8	9	5347	50	[c]	**5648**	30
	5.54		4^-	10	10	**5492**	60	[c]	**5675**	20
	5.52		5^-	10	10	5482	70	[c]	5659	20
5597	*5.58*	$h_{9/2}$ $d_{5/2}$					*88*			
	5.65		2^-	5	4	5548	40	[f]	5778	30
	5.57		3^-	9	10	5385	20	[c]	**5648**	30
	5.63		4^-	11	11	**5675**	70	[12]	**5492**	20
	5.58		5^-	11	11	*5545*	60	[12]	5659	30
	5.52		6^-	7	7	**5490**	75	[12]	5686	15
	5.56		7^-	4	4	5543	90	[12]	5694	10
5771	*5.70*	$g_{9/2}$ $f_{7/2}$					*92*			
	5.64		1^-	3	4	*5640*	90	[c]		
	5.79		2^-	6	6	5778	30	[20]	5812	30
	5.65		3^-	10	13	**5648**	40	[c]		
	5.77		4^-	12	12	5886	50	[c]	**5492**	20
	5.61		5^-	12	12	5659	50	[17]	*5545*	30
	5.67		6^-	8	8	5686	90	[17]	**5490**	10
	5.68		7^-	5	5	5694	90	[17]	5543	10
	5.83		8^-	2	2	5836	98	[17]		

TABLE I. (*Continued.*)

E_x^{SSM}	E_x^{cnt}	LJ lj	I^π	m	M	$\tilde{E}_x(1)$	c_1^2	Ref.	$\tilde{E}_x(2)$	c_2^2
5896	*5.94*[g]	$d_{5/2}$ $p_{3/2}$					*90*[g]			
	6.30[g]		1^-	4	7	6264	30	[20]	6314	50
	5.80[g]		2^-	7	7	5812	55	[20]	5778	30
	5.84[g]		3^-	11	14	5813	50	[20]	5874	30
	5.97[g]		4^-	13	14	6012	70	[20]	5886	30
5922	*5.95*	$g_{7/2}$ $p_{1/2}$					*86*			
	5.91		3^-	12	15	5874	60	[32]	6011	20
	5.97		4^-	14	13	5969	90	[32]		
5969	*5.94*	$d_{3/2}$ $p_{1/2}$					*94*			
	5.90		1^-	5	5	5947	90	[32]	5512	10
	5.96		2^-	8	8	5924	70	[32]	6087	20
6033	*5.82*	$s_{1/2}$ $f_{5/2}$					*62*			
	6.17		2^-	9	9	6087	60	[18]	6420	20
	5.52		3^-	13	11	5517	40	[c]		
6361	*6.39*	$s_{1/2}$ $p_{3/2}$					*54*			
	6.31		1^-	6	8	6314	60	[18]		
	6.44		2^-	10	10	6420	50	[18]	6552	10
6487	*6.50*	$j_{15/2}$ $i_{13/2}$								
	[h]		1^-	7	6	6076	[i]	[j]		
	[h]		2^-	11	11	6482	[i]	[14]		
	[h]		3^-	14	12	5564	[i]	[14]		
	[h]		4^-	15		[k]				
	[h]		5^-	13		[k]				
	[h]		6^-	9		[k]				
	[h]		7^-	6		[k]				
	[h]		8^-	3		[k]				
	[h]		9^-	1		[k]				
	6.28		10^-	1	1	6283	98	[14]		
	[h]		11^-	1		[k]				
	6.44		12^-	1	1	6436	98	[14]		
	6.45		13^-	1	1	6448	98	[14]		
	6.74		14^-	1	1	6743	98	[14]		
6492		$g_{7/2}$ $f_{5/2}$								
			1^-	8	9	6362	[i]	[14]		
			2^-	12	12	6552	30	[18]	6420	30
			3^-	15	16	6011	50	[5]		
			4^-	16		[k]				
			5^-	14		[k]				
			6^-	10		[k]				
6494		$f_{7/2}$ $d_{5/2}$								
			1^-	9		[k]				
			2^-	13		[k]				
			3^-	16	17	6191	[i]	[14]		
			4^-	17		[k]				
6536		$d_{3/2}$ $f_{5/2}$								

[a] A corresponding order number m is unknown.
[b] Strength of any detected configuration is small, $c^2 < 0.1$ (Sec. IV D 3).
[c] This work.
[d] Guess from complement of detectable configurations (Secs. IV D 1 and IV D 9).
[e] By including six states the centroid energies are derived as 5.03, 4.97 for spins 2^-, 3^-, respectively, 5.00 globally, and the total strength as 100% [20].
[f] The reanalysis of ^{209}Bi(d,^{3}He) data [11] shows that in the 5537 10^+, 5543 7^-, 5545 5^-, 5548 2^- doublet the 5548 2^- state contains some $h_{9/2}d_{5/2}$ strength.
[g] By including twelve states, the centroid energies are derived as 6.23, 5.81, 5.86, 5.97 MeV for spins 1^-, 2^-, 3^-, 4^-, respectively; the global centroid is determined as 5.94 MeV and the total strength as 99% [20].
[h] Ignored in the determination of E_x^{cnt}.
[i] Arbitrarily chosen configuration, unknown strength.
[j] From Ref. [14]; the spin 0^- is excluded.
[k] Not yet identified.

9^+, 11^+) in a graphical representation. In addition the multiplet splitting of several particle-hole is presented graphically and compared to the shell model.

B. Unitarity conditions

The mean value of off-diagonal matrix elements for the residual interaction among the SSM configurations is 50–150 keV [29]. For many spins, a certain set of configurations is separated from all other configurations by a gap which is large in relation to the mean value of the off-diagonal matrix elements of the residual interaction. This allows us to assume the transformation matrix $||c||$ [Eqs. (1), (4), and (5)] to be unitary, in fact orthogonal [29].

Therefore, the transformation for an ensemble of states $|\tilde{E}_x I^\pi\rangle$ to an equivalent set of configurations $LJ\,lj$ with a certain spin I^π yields the orthogonality and normality relations

$$\sum_m c^{I^\pi}_{M_i,m} c^{I^\pi}_{M_j,m} = \delta_{ij}, \tag{6}$$

and the inverse orthogonality relations and the sum rules,

$$\sum_M c^{I^\pi}_{M,m_i} c^{I^\pi}_{M,m_j} = \delta_{ij} \quad \text{where} \quad \delta_{ii} = 1 \quad \text{and} \quad \delta_{ij} = 0 \quad \text{for} \quad i \neq j. \tag{7}$$

[Note the different writing of the indices in Eqs. (1)–(5).] In reality, the orthogonality, normality relations, and the sum rules are only approximately fulfilled, hence $\delta_{ii} \approx 1$ and $\delta_{ij} \approx 0$ for $i \neq j$. The obtained precision is discussed in Sec. II E; it varies between a few percent and ignorance.

The sum rule for most configurations [Eq. (7)] becomes close to unity within 30% for most spins if only two states are considered; similarly the normalization [Eq. (6)] is mostly fulfilled within 10% if only 1–3 configurations are considered. In fact, the matrix $||c||$ [Eqs. (1)–(5)] can be described as a banded matrix,

$$\left[c^{I^\pi}_{M,m}\right]^2 = 0 \quad \text{for} \quad |M - m| > B^{I^\pi} \tag{8}$$

with bandwidth $B^{I^\pi} = 1$ or 2; most amplitudes farther off the diagonal are indeed small: $|c^{I^\pi}_{M,m}| \lesssim 0.3$ for $|M - m| > B^{I^\pi}$.

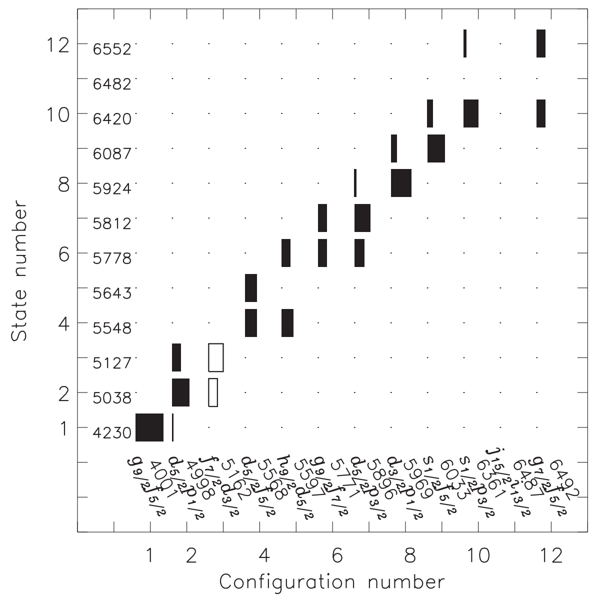

FIG. 1. Transformation matrix $||c||$ [Eqs. (1), (4), and (5)] for states in ^{208}Pb with spin 2^-. For each configuration, the order number m, the SSM energy, and the orbitals LJ and lj of the particle and the hole are given along the abscissa. The size of the rectangle shows the strength $[c_{LJ,lj}^{\tilde{E}_x I^\pi}]^2$; open rectangles denote the undetectable proton configuration $f_{7/2}d_{3/2}$.

For this reason, only two states with the leading configuration strengths are discussed in this paper. (For the spins of 1^- and 3^-, the diagonal is shifted to $M = m + 1$ because of the additional yrast state; see Sec. IV D 3.)

We do not discuss the orthogonality relations in this paper. The precision of the strengths shown in Table I is too low and the summed contribution from up to twelve configurations not discussed here may be considerable. The fit of the states at $E_x \lesssim 4.5$ MeV [29,31], however, was done with the restraining conditions of the orthonormality relations [Eqs. (6) and (7)].

Table I shows the negative parity states predicted by the SSM at $E_x < 6536$ keV and identified by NDS2007, recent Refs. [13,15–20], and this work. For each configuration (column 3) and for each spin (column 4) the two leading states bearing a major fraction of the configuration according to Eqs. (1), (4), and (5) are shown. The state with the leading configuration is shown under the heading "1. State", but the next one is not always shown. A certain state may appear up to three times if the configuration mixing is large.

Figure 1 shows the transformation matrix $||c||$ [Eqs. (1), (4), and (5)] for the lowest twelve states in ^{208}Pb with the spin of 2^-. The lowest state is rather pure while the following states are grouped into pairs with little admixture of other configurations (Table I). The bandwidth is essentially $B^{I^\pi} = 1$ [Eq. (8)] up to the state with order number $M = 9$ since all known admixtures are less than a few percent. (In Fig. 1 weak admixtures are not shown except for the admixture of configurations $d_{5/2}p_{1/2}$, $d_{5/2}p_{3/2}$ in the 4230, 5924 states, respectively [20].) Reference [25] shows transformation matrices similar to Fig. 1 for fourteen states with spin 4^- and twelve states with spin 5^-.

We prove the assumption that certain ensembles of states are described by an orthogonal transformation of an equivalent configuration space by regarding the sum of the strengths

$$S_{LJ\,lj}^{I^\pi} = \sum_i \left[c_{M_i,LJ\,lj}^{I^\pi}\right]^2 \tag{9}$$

for each configuration $LJ\,lj$ in the two leading states weighted by the spin factor $(2I + 1)$,

$$S_{LJ\,lj} = \sum_I \sum_{i=1,2} \frac{2I+1}{(2J+1)(2j+1)} \left[c_{M_i,LJ\,lj}^{I^\pi}\right]^2. \tag{10}$$

Table I shows the values.

As explained by the surface delta interaction (extending the SSM [13] in a minimal manner [21]), the centroid energy of some configurations $LJ\,lj$ (especially for the highest or lowest spin $I = |J \pm j|$) is often shifted up to several tens keV in either direction,

$$E_x^{mSM}(LJ\,lj, I^\pi) = E_x^{\rm SSM}(LJ\,lj) + \delta E_x^{\rm SDI}(LJ\,lj, I^\pi). \tag{11}$$

Here $\delta E_x^{\rm SDI}$ is calculated by the SDI [21]. It depends strongly on the Nordheim number $(-1)^{J+j+L+l}$ [33] and on the nature of the parity $(-1)^{L+l+I}$. Yet the global centroid energy for all spins is mostly close to the energy $E_x^{\rm SSM}$ in the schematic shell model without residual interaction [13,21]. (For proton configurations the Coulomb correction entering in the calculation of the SSM energies may depend on the orbital angular momenta L,l and spins J,j.)

We assume the excitation energy of a state to differ by less than about 0.2 MeV from the energy E_x^{mSM} [Eq. (11)] for the dominant configuration. Almost all known fractions of SSM configurations larger than about 10% are spread in a limited range of excitation energies $|E_x - E_x^{mSM}| \lesssim 0.2$ MeV for natural parity $[(-1)^{L+l+I} = +1]$, and $|E_x - E_x^{mSM}| \lesssim 0.1$ MeV for unnatural parity $[(-1)^{L+l+I} = -1]$.

C. Methods to determine the configuration mixing

Spectroscopic information is obtained from particle transfer reactions by the analysis of angular distributions and excitation functions.

1. *The ^{208}Pb(p,p') reaction via IAR*

Inelastic proton scattering on ^{208}Pb via IAR in ^{209}Bi yields information about the neutron particle-hole configurations in ^{208}Pb. It is equivalent to the neutron pickup reaction on a target of ^{209}Pb in an excited state. By adjusting the proton beam to a certain IAR, the neutron particle is selected.

The amplitudes $c_{LJ,lj}^{\tilde{E}_x I^\pi}$ of all neutron particle-hole configurations $LJ\,lj$ [Eq. (1)] with up to four holes lj coupled to the particle LJ corresponding to the IAR are determined from the angular distribution [34],

$$\frac{d\sigma^{(\rm p,p')}}{d\Omega}(\tilde{E}_x, I^\pi, E_p, \Theta) = \sum_K a_K(\tilde{E}_x, I^\pi, E_p) P_K(\cos\Theta), \quad K \text{ even.} \tag{12}$$

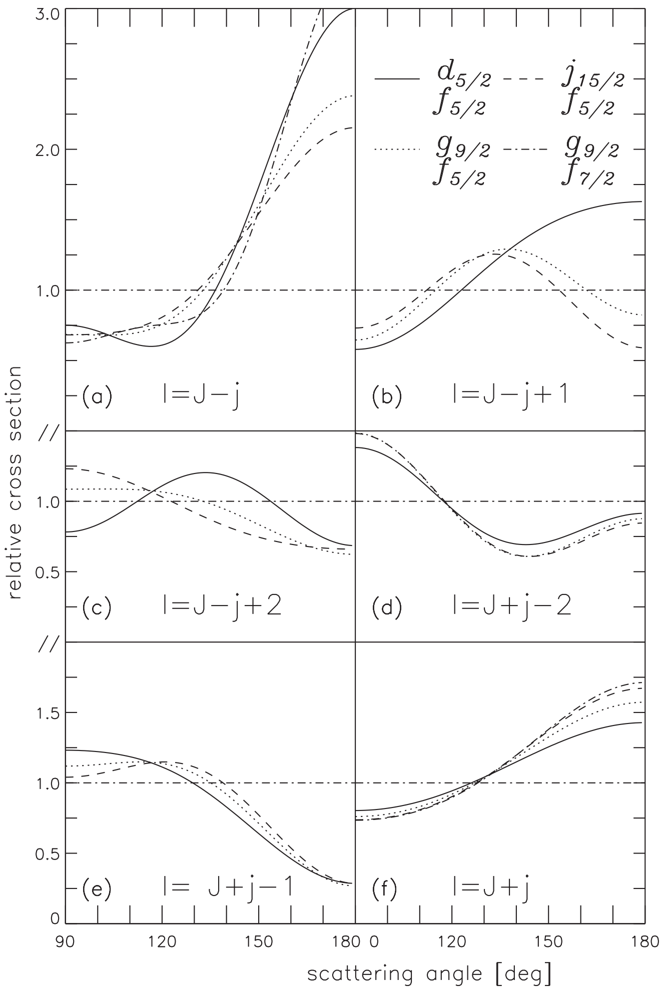

FIG. 2. Calculated angular distributions of pure particle-hole configurations $LJ\,lj$ with spins $|J-j| \leqslant I \leqslant J+j$ for $lj = f_{5/2}$ and $LJ = d_{5/2}, g_{9/2}, j_{15/2}$. Angular distributions of $g_{9/2}f_{7/2}$ for the lowest and the highest spin are shown too. The different line styles are explained in the upper right frame.

The shape of the angular distributions for the resonant ^{208}Pb(p,p') reaction is described by a series of Legendre polynomials. Figure 2 shows some typical angular distributions.

The isotropic component a_0 (the mean cross section) is proportional to the sum of the strengths c^2 [Eq. (1)] weighted by the single-particle widths [34]. Table II shows examples of calculated integral cross sections at the excitation energies $E_x = 5.2$, 5.7 MeV and the model energy $E_x^{\rm SSM}$.

The single-particle widths for outgoing protons $lj = p_{1/2}$, $p_{3/2}$ are about five times larger than for $lj = f_{5/2}$, $f_{7/2}$. Hence, admixtures of the configurations $LJ\,p_{1/2}$, $LJ\,p_{3/2}$ are determined with higher precision than admixtures of $LJ\,f_{5/2}$, $LJ\,f_{7/2}$.

Weak admixtures of configurations $L'J'\,l'j'$ of IARs $L'J'$ above the IAR LJ exciting the dominant configuration $LJ\,lj$ have enhanced cross sections due to the high penetrability of the outgoing protons $l'j'$ [35]. For example, the cross section for an admixture of $d_{5/2}p_{3/2}$ to a state with dominant configuration $g_{9/2}f_{5/2}$ is enhanced by a factor of 10.

TABLE II. Calculated cross sections $\sigma(I,LJ,lj,E_x)$ [Eq. (20)] of ^{208}Pb(p,p') for an arbitrary selection of configurations $LJ\,lj$ relevant to this paper at energy $E_x^{\rm SSM}$ and two excitation energies, $E_x = 5200$, 5700 keV. Only the value for the highest spin $I^\pi_{\rm max} = J + j$ is shown. Values for other spins I' are calculated by applying the factor $\frac{2I'+1}{2I_{\rm max}+1}$. Values for other excitation energies at $4.8 \lesssim E_x \lesssim 6.1$ MeV are approximately calculated by logarithmic interpolation, $\log_{10}\sigma(I,LJ,lj,E_x) = \frac{E_x-5200}{5700-5200}[\log_{10}\sigma(I,LJ,lj,5700) - \log_{10}\sigma(I,LJ,lj,5200)] + \log_{10}\sigma(I,LJ,lj,5200)$.

LJ	lj	$I^\pi_{\rm max}$	$E_x^{\rm SSM}$	$\sigma(I,LJ,lj,E_x)$		
			(keV)	$E_x = E_x^{\rm SSM}$ (μb/sr)	$E_x =$ 5200 keV (μb/sr)	$E_x =$ 5700 keV (μb/sr)
$g_{9/2}$	$p_{3/2}$	6^-	4329	500	210	125
$g_{9/2}$	$f_{7/2}$	8^-	5771	20	36	20
$g_{9/2}$	$i_{13/2}$	11^+	5064	3.0	2.3	0.9
$i_{11/2}$	$p_{3/2}$	7^-	5108	50	45	30
$j_{15/2}$	$f_{7/2}$	11^+	7194	1.0	4.5	3.2
$d_{5/2}$	$p_{1/2}$	3^-	4998	450	415	315
$d_{5/2}$	$f_{5/2}$	5^-	5568	120	175	120
$d_{5/2}$	$p_{3/2}$	4^-	5896	350	515	395
$d_{5/2}$	$f_{7/2}$	6^-	7338	20	90	65
$g_{7/2}$	$p_{1/2}$	4^-	5922	700	885	745

In the theoretical description of the angular distributions for the resonant (p,p') reaction [34], the shape for pure configurations $LJ\,lj$ needs several anisotropy coefficients a_K/a_0 depending on the values LJ,lj,I.

The shape of the angular distribution for pure configurations is considered to estimate the strength of each neutron particle-hole configuration (see Sec. II D). In first order, the shape of the angular distribution does not differ too much from that of the dominant configuration in the case where the admixture is not large (say a few percent), but there is no simple rule because some geometrical coefficients happen to be large. Therefore the comparison to pure configurations needs a caveat.

The anisotropy coefficients a_K/a_0 [Eq. (12)] allow us to determine the interfering amplitudes $c_{LJ,lj}^{\tilde{E}_x I^\pi}$ [Eqs. (1), (4), and (5)] if they are sufficiently precise. The sensitivity may be high as shown by the very first analysis of the 3475 4^- state by Bondorf et al. [30] yielding the amplitude of the configuration $g_{9/2}p_{3/2}$ corresponding to 8% strength in presence of the dominant $g_{9/2}p_{1/2}$ strength. The later analysis shows the admixture from $g_{9/2}f_{5/2}$, $g_{9/2}f_{7/2}$ to be less than 1% [31].

In this paper, however, we determine mean cross sections a_0 for the ^{208}Pb(p,p') reaction mostly below 30 μb/sr. A fit for such low cross sections by Legendre polynomials does not yield meaningful anisotropy coefficients a_K/a_0 for $K > 2$, often not even for $K = 2$. Instead of using Eq. (12), in some cases low mean cross sections can be determined equally well as

$$\sigma^{(\rm p,p')}(\tilde{E}_x, I^\pi, LJ) = \frac{1}{n}\sum_{i=1}^{n} \frac{d\sigma^{(\rm p,p')}}{d\Omega}\big(\tilde{E}_x, I^\pi, \Theta^i, E_p^i\big)/a^{Lz}\big(E_p^i, LJ\big). \quad (13)$$

The n values are a selection of scattering angles Θ^i and E_p^i proton energies near the chosen IAR LJ. The shape of the excitation function near the resonance is described by a Lorentzian,

$$a^{Lz}(E_p,LJ) = \frac{\left[\Gamma_{LJ}^{\rm tot}\right]^2}{4\left(E_p - E_{LJ}^{\rm res}\right)^2 + \left[\Gamma_{LJ}^{\rm tot}\right]^2}. \quad (14)$$

The resonance energies $E_{LJ}^{\rm res}$ and total widths $\Gamma_{LJ}^{\rm tot}$ determined by Wharton *et al*. [5] are used.

The mean cross section [Eq. (13)] often deviates by a large factor from the isotropic component of the fit by Legendre polynomials because of the lack of data taken at scattering angles far from 90°, either $150^\circ \lesssim \Theta < 180^\circ$ or $\Theta \lesssim 30^\circ$. In addition, the direct-(p,p') reaction often contributes considerably at scattering angles $\Theta \lesssim 90^\circ$. Therefore, if possible, we choose $\Theta \gtrsim 90^\circ$ for the determination of cross sections in order to avoid contributions from the direct (p,p') reaction.

2. The neutron transfer reaction ^{207}Pb(d,p)

For the ^{207}Pb(d,p) reaction, spectroscopic factors proportional to the strength $|c_{LJ,p_{1/2}}^{\tilde{E}_x I^\pi}|^2$ are obtained by comparison to distorted-wave Born approximation (DWBA) calculations [32],

$$S_{LJ}(\tilde{E}_x,I^\pi) = \frac{1}{n}\sum_{i=1}^{n}\frac{d\sigma}{d\Omega}(\tilde{E}_x,I^\pi,\Theta^i)\Big/\frac{d\sigma^{DWBA}}{d\Omega}(\tilde{E}_x,\Theta^i,LJ) \quad (15)$$

for some orbital angular momentum L and spin $J = L \pm \frac{1}{2}$ of the particle; the hole is $p_{1/2}$.

The sum should be extended to take different LJ values into account, but the incoherent sum of the angular distributions is determined only with difficulty. The angular distributions of the analyzing power often assist in differentiating mixtures of two LJ values [32].

For low cross sections, the mean cross section is compared to strongly excited states with known spectroscopic factors. For the ^{207}Pb(d,p) reaction it is determined as

$$\sigma^{\rm (d,p)}(\tilde{E}_x,I^\pi) = \frac{1}{n}\sum_{i=1}^{n}\frac{d\sigma^{\rm (d,p)}}{d\Omega}(\tilde{E}_x,I^\pi,\Theta^i), \quad 15^\circ \leqslant \Theta^i \leqslant 30^\circ. \quad (16)$$

The strengths of the configurations $LJp_{1/2}$ were determined from the ^{207}Pb(d,p) experiments with polarized deuterons [32] and with unpolarized deuterons [15,36]. The contribution of two values, LJ and $L'J'$, to the cross section in each state was determined from the angular distribution of the cross section. Depending on the spin I of the state, the orbital angular momenta L,L' are the same or $L' = L + 2$ or $L' = L - 2$. The ^{207}Pb(d,p) reaction with polarized deuterons determined in many cases components with spin $J = L + \frac{1}{2}$ and $J' = L' - \frac{1}{2}$ from the angular distribution of the analyzing power [32].

3. The proton transfer reactions ^{209}Bi$(d,^3$He), ^{209}Bi$(t,\alpha\gamma)$

The strengths of the proton particle-hole configurations $h_{9/2}lj$ were determined from the ^{209}Bi$(d,^3$He) experiment [10] similarly as for ^{207}Pb(d,p) by

$$S_{lj}(\tilde{E}_x,I^\pi) = \frac{1}{n}\sum_{i=1}^{n}\frac{d\sigma}{d\Omega}(\tilde{E}_x,I^\pi,\Theta^i)\Big/\frac{d\sigma^{\rm DWBA}}{d\Omega}(\tilde{E}_x,\Theta^i,lj). \quad (17)$$

Here the hole has orbital angular momentum l and the particle is $h_{9/2}$. Different lj values may contribute, but only admixtures of $d_{3/2}$ to states with dominant $s_{1/2}$ components were determined [10,12]. The contributions from configurations with $lj = d_{3/2}$ and $d_{5/2}$ are distinguished by the SSM energy; $l = 2$ strength in states at $E_x < 4.9$, $E_x > 4.9$ MeV is assigned as $h_{9/2}d_{3/2}$, $h_{9/2}d_{5/2}$, respectively.

The resolution of about 15 keV in the ^{209}Bi$(d,^3$He) experiment is insufficient to resolve many states in the region $4.6 < E_x < 6.0$ MeV. Especially the dense ensemble of eleven states within 75 keV at $E_x \approx 5.7$ MeV, from the 5640 1^- to the 5715 2^+ state, is not properly resolved.

Still available data from the ^{209}Bi$(d,^3$He) experiment performed in 1981 were reanalyzed [11]. Spectroscopic data for the ensemble of states neighboring the 5675 state is determined and used in Secs. IV C, IV D 8.

The ^{209}Bi$(t,\alpha\gamma)$ experiment determined excitation energies with a typical uncertainty of 0.3 keV [12]. It relates the number of coincidences $S_{\rm rel}$ to the spectroscopic factor S_l determined by the ^{209}Bi$(d,^3$He) experiment through the normalization to values for states assumed to be correctly identified.

4. Undetectable configurations

Undetectable configurations are determined as the complement in a matrix of configurations describing an equivalent number of states. In case the matrix may be assumed to be orthogonal [Eqs. (6) and (7)], the strength of undetectable configurations can be determined with sufficient precision.

Some unnatural parity states build pairs which may be assumed to contain essentially only two configurations. The strength of an undetectable configuration in the pair can be rather well determined. The complete $f_{7/2}d_{3/2}$ strength has been thus determined in the 5239 4^-, 5276 4^- states with a mixing ratio of 9 : 1 [15]. Similarly, the 5038 2^-, 5127 2^- states essentially contain only $d_{5/2}p_{1/2}$, $f_{7/2}d_{3/2}$ strengths (Table I, Fig. 1).

5. Centroid energies

The centroid energy for the configuration $LJ\,lj$ is determined by

$$E_x^{\rm cnt}(LJ,lj,I^\pi) = \sum_{\tilde{E}_x}\tilde{E}_x\big[c_{LJ,lj}^{\tilde{E}_x I^\pi}\big]^2\Big/\sum_{\tilde{E}_x}\big[c_{LJ,lj}^{\tilde{E}_x I^\pi}\big]^2 \quad (18)$$

for each spin I^π and globally by

$$\overline{E_x^{\rm cnt}}(LJ,lj) = \frac{\sum_I(2I+1)\sum_{\tilde{E}_x}\tilde{E}_x\big[c_{LJ,lj}^{\tilde{E}_x I^\pi}\big]^2}{\sum_I(2I+1)\sum_{\tilde{E}_x}\big[c_{LJ,lj}^{\tilde{E}_x I^\pi}\big]^2}. \quad (19)$$

D. Methods of spin and parity assignment by particle spectroscopy

The analysis of states in ^{208}Pb indicates that seldom more than four configurations are needed to fulfill the normalization rule [Eq. (6)] by more than 90%; for states with unnatural parity mostly two configurations suffice [13,15–18,20]. Similarly, the strengths of a certain configuration in less than four states fulfill the sum rule [Eq. (7)] by more than 90%.

Inelastic proton scattering via IAR allows us to determine amplitudes of neutron particle-hole configurations including their sign, not only the strength (the squares of amplitudes) [34]. The orthogonality relations [Eq. (7)] then allow us to favor certain spin assignments to pairs of states consisting essentially of two configurations. Here, small admixtures have to be determined precisely since a few 1% admixtures may add up to a 10% effect. The spin assignments for the 4262, 4359 4^- pair and the 4363, 4481 6^- pair consisting essentially of the two configurations $h_{9/2}d_{3/2}$ and $g_{9/2}p_{3/2}$ were thus found [29]; the spin assignments are now confirmed [14,31]. More sophisticated usage of the orthogonality relations relies on the knowledge of the sign of certain amplitudes which can be determined from precisely measured angular distributions of ^{208}Pb(p,p') via IAR [9]. This method has been used to determine the spins of the states at $E_x < 4.5$ MeV [29,31]. We do not discuss this method further, and we do not use this method here.

Particle spectroscopy offers several methods to determine spin and parity. The determination of the parity relies on the knowledge of the participating valence nucleons in particle-hole states. In case of the ^{208}Pb(p,p') reaction via IAR in ^{209}Bi, only the $j_{15/2}$ IAR excites positive parity states with a significant resonance behaviour. All other states with clear resonances in the excitation function at the known IARs have negative parity.

For some states not excited significantly by any IAR and showing a smooth excitation function, the direct-(p,p') reaction is dominant. These states have positive parity and mostly low spins (0^+ - 4^+).

In some doublets one state is excited by the direct-(p,p') reaction and another one resonantly. Even if the excitation energies of the two members of the doublet cannot be distinguished, clearly the parity of the IAR defines the parity of one member. Thus the 4.93, 5.19, 5.21, and 5.99 MeV doublets are disentangled [13]; see also Sec. III C.

In case of the ^{207}Pb(d,p) and ^{209}Bi$(d,{}^3$He) reactions, the unambiguous determination of the orbital angular momentum of the emitted nucleon (L, l) corresponding to the intruder valence nucleon, $j_{15/2}$, $h_{11/2}$, respectively, indicates positive parity [10–12,32].

The integral cross section of a certain configuration $LJ\,lj$ is split into parts where the particle LJ is coupled to the hole lj yielding the spins $|J-j| \leqslant I \leqslant J+j$. Hence, the integral cross section of a state with configuration $LJ\,lj$ and spin I is proportional to the spin factor $(2I+1)$,

$$\sigma(I,LJ,lj,E_x) = \frac{2I+1}{2J+1}\sigma_0(LJ,lj,E_x) \qquad (20)$$

with the sum [37]

$$\sum_{I=|J-j|}^{J+j}(2I+1) = (2J+1)(2j+1). \qquad (21)$$

The cross section σ_0 can be calculated for the ^{208}Pb(p,p') reaction, especially the ratios for different IARs LJ are reliably known. Because the calculated values are uncertain by 10%–20%, the cross section σ_0 is determined in an iterative manner from experimental data by using the normality and sum rule relations [Eqs. (6) and (7)].

The cross section σ_0 varies strongly with the difference between the energy $E_x^{\rm SSM}$ of the dominant configuration and the excitation energy of state; the penetrability of the outgoing protons, however, is reliably calculated [35]. Table II shows cross sections calculated with experimentally determined single particle widths for three excitation energies.

Figure 2 shows angular distributions for $lj = f_{5/2}$ with $LJ = d_{5/2}$, $g_{9/2}$, $j_{15/2}$ and spins $|J-j| \leqslant I \leqslant J+j$ and in frames (a) and (f) with two angular distributions for $g_{9/2}f_{7/2}$, $I = J-j$ and $J+j$; different values LJ,lj denoted by different line styles are explained in frame (b).

The highest degree of the contributing [always even] Legendre polynomials in the angular distribution for a state containing several configurations $LJ\,lj$ [Eq. (1)] is given by the minimal value of $2L$,$2J$, max$(2l)$, max$(2j)$ [34]. Thus, for $lj = p_{1/2}$ and $LJ = s_{1/2}$ an isotropic angular distribution is expected. For $lj = p_{3/2}$ the angular distributions for spins $I = |J \pm j|$ have a deep minimum at $\Theta = 90^\circ$; for the other two spin values there is a pronounced maximum at $\Theta = 90^\circ$. For higher values L,J,l,j the shape of the angular distribution assumes more complicated features, but for the highest and lowest spin I there is always a deep minimum at $\Theta = 90^\circ$.

The angular distributions for $I = |J-j|$ have a steeper raise near $\Theta = 0^\circ, 180^\circ$ than for $I = J+j$. The lowest 2^- state and the 7^- state with dominant configurations $g_{9/2}f_{5/2}$ are thus recognized [29]; similarly the two lowest 8^- states with configurations $i_{11/2}f_{5/2}$, $g_{9/2}f_{7/2}$ $(I = J+j)$ [15,17]. The 5615 state with dominant configurations $j_{15/2}p_{3/2}$ is assigned the spin of 7^+ since the spin of 9^+ has a distinctive opposite anisotropy of the angular distribution [13] $(I = J-j+1$ and $I = J+j)$.

The angular distributions of the 4712 4^-, 4761 6^-, 4680 7^-, 4919 8^- states with dominant configuration $i_{11/2}f_{5/2}$ and the angular distributions of the 5276 4^-, 5075 5^-, 5080 6^-, 5085 7^- states with dominant configuration $i_{11/2}p_{3/2}$ show little contributions of other configurations with the $i_{11/2}$ particle [15]. Similarly, the angular distributions of the 5^-, 6^-, 7^-, 8^- states with dominant configuration $g_{9/2}f_{7/2}$ show little contributions of other configurations with the $g_{9/2}$ particle [17].

The 5813 3^- state with a large $d_{5/2}p_{3/2}$ component explains the large anisotropy of the angular distribution of the 5.81 MeV doublet [20]. Namely, the anisotropy for the 5812 2^- state with a large $d_{5/2}p_{3/2}$ component is flat (predicted as $a_2/a_0 = -0.114$ with $I = J-j+1$) while it is extremely pronounced for the 5813 3^- state (predicted as $a_2/a_0 = -0.629$ with $I = J+j-1$; see also Fig. 2). The measured anisotropy $a_2/a_0 = -1.03 \pm 0.05$ [9] indicates weak admixtures of other configurations with a $d_{5/2}$ particle to both states. (The observed variation of the shift in the centroid excitation energy with scattering angle [20] can be explained by the different anisotropies in the incoherent superposition of the angular distributions too).

The integral cross section for the ^{208}Pb(p,p') reaction is determined with a large uncertainty if the range of scattering angles is limited. One must always inspect the shape predicted for the pure configuration (see Fig. 2) and keep in mind distortions by the interference with weak admixtures of other configurations while comparing the mean cross section $\sigma^{(\mathrm{p,p'})}$ to calculated integral cross sections (see Table II).

The contribution of the direct-(p,p') reaction introduces another complication. For some states, the cross section of the direct-(p,p') reaction exceeds the resonant cross section largely at scattering angles $\Theta \lesssim 100^\circ$.

In the case where good angular distributions both at backward angles $\Theta = 90^\circ$–170° and forward angles $\Theta \leqslant 90^\circ$ are available, the contribution of the direct-(p,p') reaction can be estimated. As an example, the 6011 3^- state (in the doublet with the 6012 4^- state) is strongly excited by the direct-(p,p') reaction at $\Theta \lesssim 90^\circ$ [9,20].

Excitation functions for the ^{208}Pb(p,p') reaction reveal the resonant excitation on certain IARs in ^{209}Bi. By comparing the integral cross section to calculated values (Table II), a range of spins is assigned to each state. The method has been applied to assign new spins for states with major fractions of the configurations $d_{5/2}p_{1/2}$ and $d_{5/2}p_{3/2}$ [20].

In the case where two IARs excite a certain state, the overlap of the range of possible spins may leave only one spin. An example is the excitation of the 4698 3^- state with major fractions of $g_{9/2}p_{3/2}$ and $d_{5/2}p_{1/2}$. (The early measurement [3] did not resolve the 4698 3^- state from the 4709 5^-, 4712 4^- states in the doublet. These states have low cross sections on the $g_{9/2}$, $d_{5/2}$ IARs as they consist mostly of the configuration $i_{11/2}f_{5/2}$ [15].)

For the ^{207}Pb(d,p) reaction the range of spins is restricted to $I = J \pm \frac{1}{2}$, since the ground state of ^{207}Pb has spin 1/2. The ^{207}Pb(d,p) reaction with polarized deuterons yields different angular distributions of the analyzing power with spin $J = L + \frac{1}{2}$ and $J' = L' - \frac{1}{2}$, where the two orbital angular momenta L, L' may be the same or different. By this means several spins are assigned, especially the spin of 4^- to the 5886 state [20].

The low resolution for the ^{209}Bi$(d,{}^3$He$)$ reaction (about 15 keV) hinders the identification of the states; the ^{209}Bi$(t,\alpha\,\gamma)$ reaction assists in resolving doublets. Nevertheless spin assignments for some states are undoubted if there are no neighbors in less than about 15 keV distance, e.g., the 3947 4_2^-, 3961 5_3^- states [10]. The isolation of the 5675 state from the neighbors corroborates the assignment of spin 4^- by Schramm *et al.* [10–12].

Equation (20) can be used to exclude assignments of a low spin by the cross section being too high. This method is especially useful to determine the highest spins of some configuration $LJ\,lj$. Namely, the ratio $\frac{2I+1}{2J+1}$ spans a range that is wider for a larger spin of the valence nucleon j. By this means the spins 1^-, 2^-, 3^-, 4^- have been excluded for the states with dominant configuration $g_{9/2}f_{7/2}$ excited on the $g_{9/2}$ IAR at $5.6 < E_x < 5.9$ MeV [17].

Another application of Eq. (20) is possible since the penetrability of $p_{1/2}$, $p_{3/2}$ protons is about five times higher than for $f_{5/2}$, $f_{7/2}$ protons. Cross sections larger than the maximum for the configuration $LJ\,f_{5/2}$ restrict the range of spins to $I \leqslant |J \pm \frac{3}{2}|$, or to $I \leqslant |J \pm \frac{1}{2}|$ if the ^{207}Pb(d,p) reaction is dominant. The 6420 2^- state has been thus identified [18].

Weak cross sections in the ^{208}Pb(p,p') reaction may offer an unusual tool because of the progressive penetrability of the scattered proton. As Table II indicates, weak admixtures of distant configurations become enhanced by large factors if the excitation energy of the state is much lower than the SSM energy of the configuration. Enhancements by a factor of 10 may occur. In Sec. III D a weak $j_{15/2}f_{7/2}$ admixture to the 5235 11^+ state is deduced. (Similarly, the clear resonant excitation of the 3198 5_1^- state on the $d_{5/2}$ IAR [3] is explained by about 1% $d_{5/2}f_{5/2}$ and 0.2% $d_{5/2}f_{7/2}$ admixtures.)

Weak admixtures often are the only means to determine the structure of states with major undetectable configurations by regarding the orthogonality relations; see Sec. III D for the 4911 4^-, 4937 3^- states with dominant configuration $f_{7/2}s_{1/2}$, and Sec. IV D 9 for the $f_{7/2}d_{3/2}$ configuration.

E. Determining configuration strengths

Configuration strengths can be determined from the study of the ^{207}Pb(d,p) and ^{209}Bi$(d,{}^3$He$)$ reactions and the inelastic proton scattering on ^{208}Pb via IAR in ^{209}Bi.

The angular distributions of the ^{207}Pb(d,p) reaction with polarized deuterons [32] and with unpolarized deuterons [15,36], the angular distributions of the ^{209}Bi$(d,{}^3$He$)$ reaction [10], and the coincidences of the ^{209}Bi$(t,\alpha\,\gamma)$ reaction in comparison to the results from the ^{209}Bi$(d,{}^3$He$)$ reaction [12] allowed us to determine the strengths $[c_{LJ,lj}^{\tilde{E}_x I^\pi}]^2$ for the configuration $LJ\,lj$ in a state $|\tilde{E}_x I^\pi\rangle$ [Eqs. (15) and (17)]. The uncertainty of the strength relies on the comparison to DWBA calculations; a relative precision of about 10% can be achieved.

The analysis of the angular distributions and excitation functions of the resonant ^{208}Pb(p,p') reaction allow us to determine the strengths of neutron particle-hole configurations [13,15–20]; see Eqs. (12) and (13). In principle even the amplitudes itselves together with their signs can be determined [34]; yet in this paper we do not use this information.

The high sensitivity of the Q3D magnetic spectrograph allows us to detect weak cross sections. Thus configuration strengths down to $c^2 = 0.1\%$ [Eqs. (1) and (15)] can be deduced from the ^{207}Pb(d,p) reaction. Weak cross sections of the ^{208}Pb(p,p') reaction down to 0.5 μb/sr may also yield small strengths of neutron particle-hole configurations; here the large span of the penetrability factors has to be regarded (Table II).

The uncertainty of the strength varies largely. Generally, configuration strengths near 100% mean that the given SSM configuration is dominant and no large admixtures are present. Strengths of $c^2 = 90\%, 95\%, 98\%$ [Eqs. (1), (4), and (5)] in Table I indicate that the sum of the admixtures from all other configurations is less than $10 \pm 5, 5 \pm 3, 2 \pm 1\%$, respectively;

TABLE III. Excitation energies E_x, spin I, parity π, and order number M of states containing major fractions of undetectable particle-hole configurations (and close neighbors) from the ^{208}Pb(p,p') and ^{207}Pb(d,p) reactions. Doublets with distances less than about 2 keV between the states are marked by vertical lines. Energy labels of states with new spin and parity assignments are printed boldface, and confirmed or verified assignments in italics.

$\tilde{E}_x$	I^π_M	Note	NDS2007 [14]		^{208}Pb(p,p')	^{207}Pb(d,p)
			I^π	E_x (keV)[a]	E_x (keV)[b]	E_x (keV)[b]
4911	4^-_7	c,d	4^-	4911.343 ± 0.020	4911.4 ± 0.2	4911.4 ± 0.8
4937	3^-_5	c,d	3^-	4937.19 ± 0.04	4937.2 ± 0.1	4937.3 ± 0.5
4953	3^+_1	c	3^-	4953.302 ± 0.017	4953.3 ± 0.3	e
5193	5^+_2	c,d	5^+	5193.428 ± 0.025	5193.8 ± 0.6	e
5195	3^-_7	c	3^-,4^-	5195.054 ± 0.023	5194.8 ± 0.1	5194.9 ± 0.1
5196	7^+_3	c,d	7^+	5195.37 ± 0.10	5195.4 ± 0.2	5195.2 ± 0.2
5213	6^+_3	c,d	6^+	5213.007 ± 0.021	5213.1 ± 0.4	e
5214	5^-_9	c	(5^-)	5213.98 ± 0.03	5214.2 ± 0.2	5213.8 ± 0.5
5216	4^+_2	c,d	4^+	5216.214 ± 0.018	5215.8 ± 0.4	e
5235	11^+_1	c	(11^+)	5235.37 ± 0.11	5235.9 ± 0.5	e
5383	4^+	c	3^+,4^+,5^+	5382.82 ± 0.03	5382.8 ± 0.4	e
5385	3^-_x	c,d	3^-	5384.59 ± 0.03	5384.6 ± 0.2	5384.7 ± 0.5
5490	6^-_7	c	$(4^-,6^-)$	5490.34 ± 0.05	5490.4 ± 0.2	e
5492	4^-_{10}	c	$(4^-,6^-)$	5491.53 ± 0.03	5491.7 ± 0.2	5491.6 ± 0.5
5640	1^-_4	c,d	1^-	5639.55 ± 0.09	5639.4 ± 0.5	5639.8 ± 0.8
5642	2^+	c	$1,2^+$	5641.98 ± 0.20	5642.4 ± 0.3	e
5643	2^-_5	c	2^- - 7^-	$5643. \pm 4$	5643.2 ± 0.1	e
5648	3^-_{14}	c	3^-,4^-	5649.01 ± 0.06	5648.8 ± 0.3	5648.5 ± 1.0
5649	9^+_4	c	6^+ - 9^+	5649.5 ± 0.4	5649.4 ± 0.2	e
5675	4^-_{11}	c	2^-,3,4	5675.366 ± 0.023	5675.5 ± 0.2	5675.5 ± 0.5

[a]Mostly the systematic and not the experimental uncertainty is given [39].
[b]This work.
[c]Section IV C.
[d]NDS2007 [14].
[e]Not observed; see Table IV.

for strengths lower than 80% the relative uncertainty is mostly in the order of 10%–30%. Yet, small admixtures (0.1%–10%) are often precisely determined as mentioned several times in Sec. IV.

The sum rule and normality relations [Eqs. (6) and (7)] generally yield a value less than unity since only the two or three major components are considered. In the case where more than two configurations contribute with at least 20% strength each, then the sum rule and normality relations may deviate from unity by about 30%.

The orthogonality relations are investigated too, but the deviations $\delta_{ij}, i \neq j$, from zero [Eq. (7)] are only roughly approximated. Small values may add up coherently and thus yield large deviations of δ_{ij} from zero. (Note that the resonant ^{208}Pb(p,p') reaction is sensitive to the signs of the amplitudes; they thus can be determined from the angular distributions [34].)

For states dominantly excited by the ^{208}Pb(p,p') reaction on a certain IAR LJ, small admixtures from particle-hole configurations built with particles in higher orbits $L'J'$ $[E_x^{\mathrm{SSM}}(L'J') > E_x^{\mathrm{SSM}}(LJ)]$ have cross sections largely enhanced by the increased penetrability of the outgoing protons. Therefore very small admixtures can be reliably determined, often for strengths down to 0.1%.

III. EXPERIMENTAL DATA

A. Resolution, peak shape, and doublets

In the region $4.8 < E_x < 6.1$ MeV, the mean distance between neighboring states is about 10 keV while the resolution in particle spectroscopy is 3–15 keV. The minimal distances between any two states are observed for the 5195 3^-, 5196 7^+ doublet (Table III) and for the 5812 2^-, 5813 3^- doublet [20] with 0.3–0.4 keV.

We define a doublet as a group of states which is not resolved by some experiment. Especially experiments with the Q3D magnetic spectrograph yield a mean resolution of 3 keV. In this paper, hence, we limit the region of a doublet to about 2 keV. The term "multiplet" is reserved for a particle-hole configuration split into its different spin members [20].

The peak shape in ^{207}Pb(d,p) and ^{208}Pb(p,p') experiments with the Q3D magnetic spectrograph is asymmetric. In Figs. 3–10 the dashed vertical line at each peak denotes the position of the Gaussian by the fit with GASPAN [38] followed by an exponential tail (see Appendix A in Ref. [13]).

For ^{208}Pb(p,p') via IAR in ^{209}Bi, an average resolution of 1.5 keV HWHM is obtained on the low excitation energy

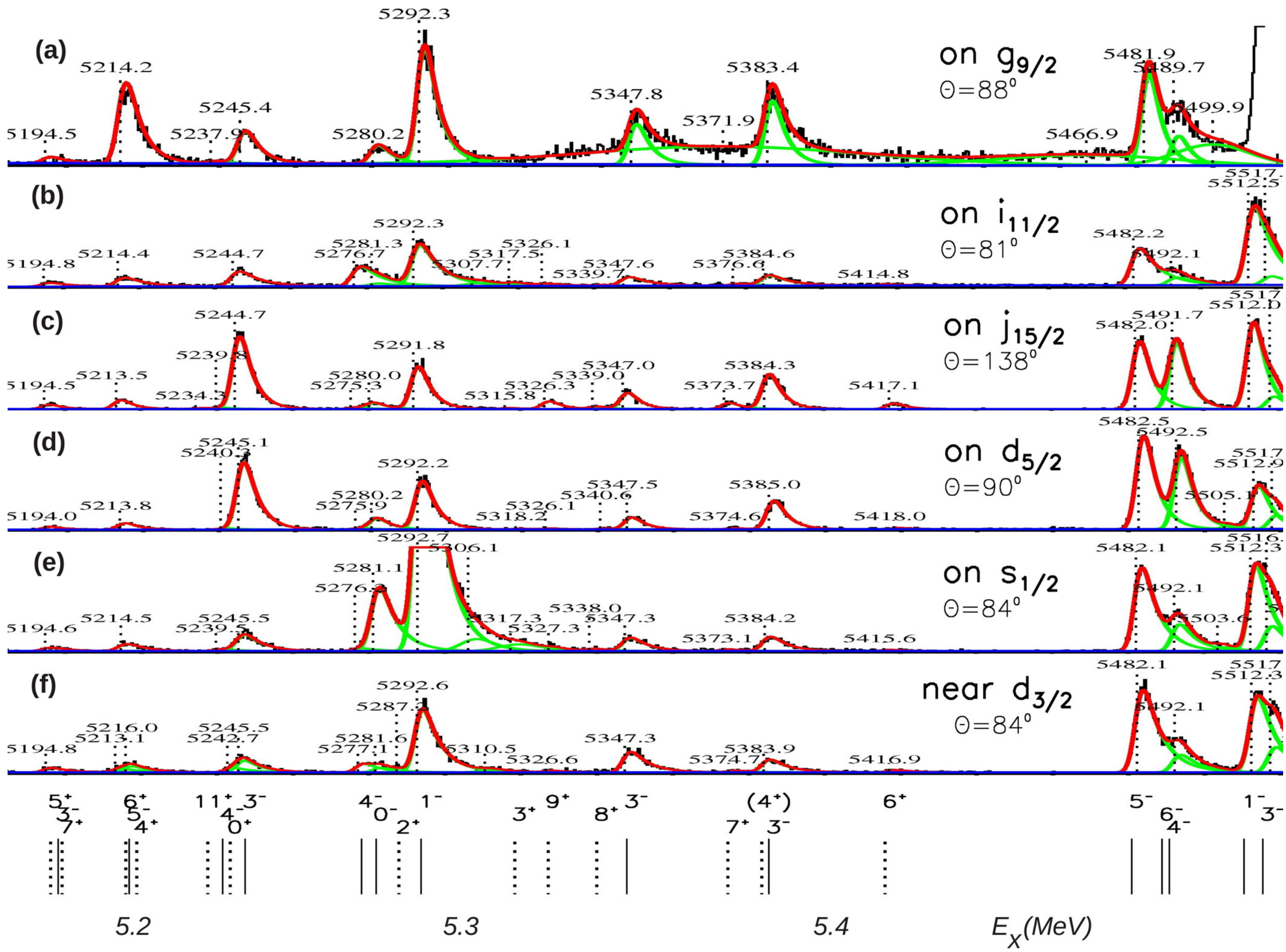

FIG. 3. (Color online) Excerpts of spectra from ^{208}Pb(p,p') via IAR in ^{209}Bi for $5.18 < E_x < 5.51$ MeV. For details see Sec. III B.

side, for ^{207}Pb(d,p) about 1.7 keV. (A few spectra taken with thinner targets yield a resolution of 1.3 keV HWHM.)

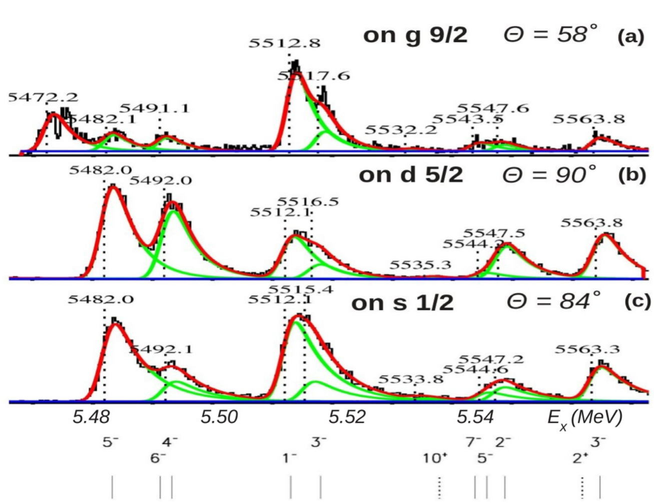

FIG. 4. (Color online) Excerpts of spectra from ^{208}Pb(p,p') via IAR in ^{209}Bi for $5.46 < E_x < 5.57$ MeV. For details see Sec. III B.

On the high energy side, each peak is followed by a series of satellites from the knockout of L electrons [13,22]; the binding energies are $E_B = 13$–15 keV. Tails from L electrons are visible in Fig. 3 for the 5292 1^- peak at 5.31 MeV, in Fig. 5 at 4.10 MeV, in Fig. 6 at 4.73 MeV, in Fig. 7 at 4.72, 4.74, 4.86, 4.88, 4.99 MeV, in Fig. 8 at 5.05, 5.31 MeV, in Fig. 9 at 5.50, 5.53, 5.82 MeV, and in Fig. 10 at 5.98, 6.11 MeV.

The length of the tail depends on the position and angle of the target foil, whether the carbon backing is traversed, and on the scattering angle. The M electrons with binding energies $E_B = 2.48$, 2.59, 3.07, 3.55, 3.85 keV finally limit the resolution.

Because of the asymmetric peak shape, doublets with a distance of about 1 keV are resolved if the state with the lower excitation energy is more weakly excited. Doublets with a distance of less than 1 keV can be disentangled if the cross sections of the states differ much when going from one IAR to another IAR or between the ^{207}Pb(d,p) and ^{208}Pb(p,p') reactions. An example is given by the 5490 6^-, 5492 4^- doublet (Sec. III C, Tables III and IV, Fig. 4).

Several doublets with a distance of less than 1 keV are thus recognized [13,15–20]. In this paper six more 2-keV doublets are discussed (Secs. III C and IV C). Table III shows

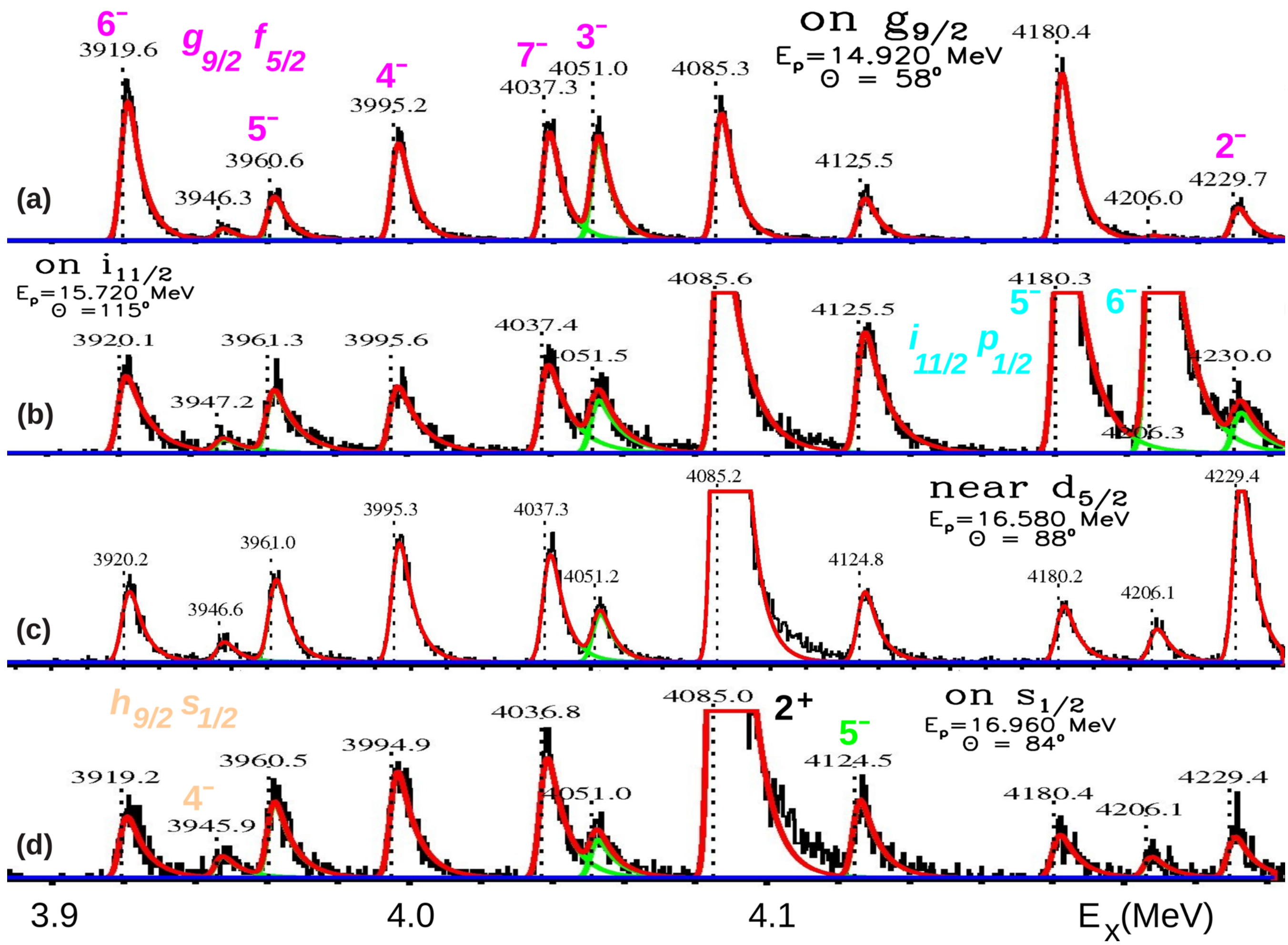

FIG. 5. (Color online) Excerpts of spectra for $3.91 < E_x < 4.24$ MeV (a) on the $g_{9/2}$ IAR, (b) on the $i_{11/2}$ IAR, (c) near the $d_{5/2}$ IAR ($E^{\mathrm{res}} = 16.496$ MeV [5]), and (d) on the $s_{1/2}$ IAR. The states with dominant $g_{9/2} f_{5/2}$ components are marked in frame (a), the states with dominant $i_{11/2} p_{1/2}$ components in frame (b), and the 4^- state with a dominant proton configuration $h_{9/2}s_{1/2}$ component and the 4086 2^+ state in frame (d). (The 3708 5^- and 3961 5^- states contain the major $h_{9/2}s_{1/2}$ 5^- strength.) Satellites from the electron knockout reaction [13] are especially observed for the 4085 2^+ state. For more details see Sec. III B.

the excitation energies, Table IV the cross sections. In addition, four weakly excited states with distances of 4–12 keV from stronger excited states are discussed.

The linearity of the Q3D magnetic spectrograph is high; the energies are effectively fitted by a polynomial of fourth degree [13]. For many states the uncertainty of the excitation energy is determined as 0.1 keV by the ^{207}Pb(d,p) and the ^{208}Pb(p,p') reactions. It derives from statistics and varying methods of background substraction.

B. Spectra for ^{208}Pb(p,p')

Spectra are shown to exemplify the quality of the data. The main objective is to show the resolution of states. The ordinates representing counts are not shown. Namely because the angular distribution of a certain state is often steep [see typical examples in Fig. 2(a)] and the counting rate on different IARs may vary by a factor hundred, the comparison of spectra is difficult.

All spectra shown in this work are fitted by GASPAN [38]. For clarity, not all levels were treated by GASPAN. Each level is followed by broader peaks produced by the electron knockout reaction [13]. Section III A lists the levels produced by the knockout of L electrons with a binding energy of about 15 keV in Figs. 3–10. In Figs. 3(a) and 4(a), contaminations from light nuclei are present in the spectra taken on the $g_{9/2}$ IAR. The other spectra are selected to contain no such contamination lines.

Figure 3 shows spectra for ^{208}Pb(p,p') in the region $5.18 < E_x < 5.51$ MeV taken on the lowest five IARs in ^{209}Bi ($E_p = 14.920$, 15.720, 16.390, 16.495, 16.960 MeV) and at $E_p = 17.610$ MeV near the $g_{7/2}$ and $d_{3/2}$ IARs ($E^{\mathrm{res}} = 17.430$, 17.476 MeV, respectively [5]). It starts with the weak doublet consisting of the 5193 5^+, 5195 3^-, 5196 7^+ states followed by some prominent selective excitations. We mention the 5215 5^- state more strongly excited on the $g_{9/2}$ IAR with its close neighbors 5213 6^+, 5216 4^+; the 5245 3^- state more strongly excited on the $d_{5/2}$ IAR with its close neighbors 5235 11^+, 5239 4^-, 5241 0^+; the prominent 5280 0^-, 5292 1^- states on

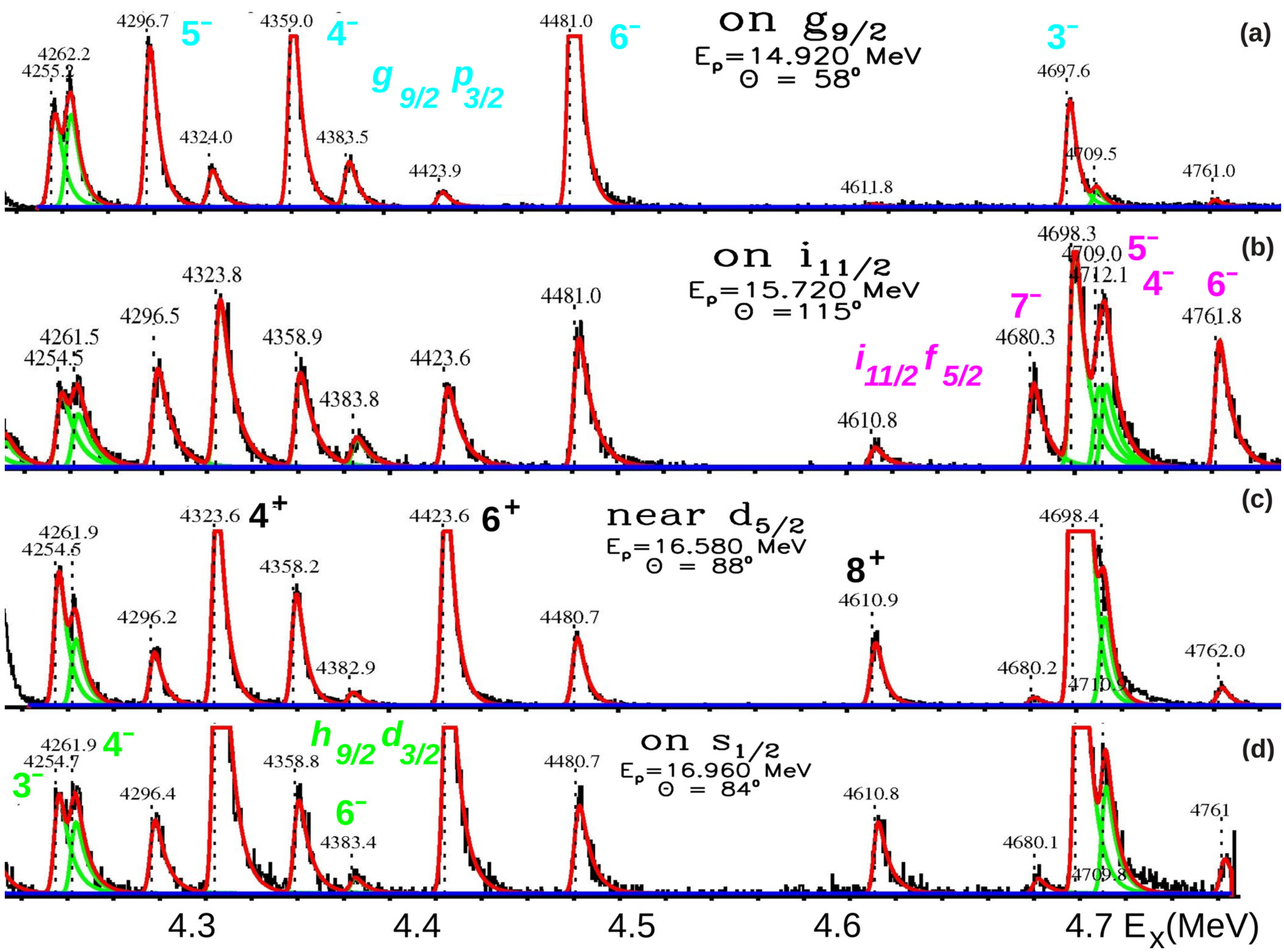

FIG. 6. (Color online) Continuation of Fig. 5 for $4.24 < E_x < 4.77$ MeV. [In frame (d), the end of the spectrum is distorted.] The states with dominant $g_{9/2}p_{3/2}$ and $i_{11/2}f_{5/2}$ components are marked in frames (a) and (b), and the states with the dominant proton configuration $h_{9/2}d_{3/2}$ in frame (d); for the 5^- member see Fig. 5. The 4324 4^+, 4424 6^+, 4611 8^+ states are marked in frame (c). Satellites from the electron knockout reaction [13] are especially observed for the 4698 3^- state. For more details see Sec. III B.

the $s_{1/2}$ IAR with the 5286 2^+ in between; the 5347 3^-, 5385 3^- states surrounded by the 5326 9^+, 5339 8^+, 5374 7^+, 5419 6^+ states more strongly excited on the $j_{15/2}$ IAR; the 5482 5^- state; the 5490 6^- state more strongly excited on the $g_{9/2}$ IAR; the 5492 4^- state more strongly excited on the $d_{5/2}$ IAR; finishing with the 5512 1^- state at the edge of the spectra, close to the 5517 3^- state.

Doublets at $E_x = 5.19$, 5.21, 5.49 MeV are discussed in Secs. III C and IV C; doublets at $E_x = 5.24$, 5.29 MeV are discussed elsewhere [13,15,16,18–20].

Figure 4 starts with the 5482 5^- state. (On the $g_{9/2}$ IAR [frame (a)], a 0.3 MeV broad line from ^{12}C(p,p') ends near $E_x = 5.47$ MeV, deteriorated by the incomplete detection in the first 17 channels at the edge of the detector.) The 5512 1^-, 5517 3^- states are fully resolved. In these spectra, the 5548 2^- state is not clearly resolved from the 5543 7^-, 5545 5^- states, and the 5561 2^+ state not from the 5564 3^- state.

The 5490 6^- state is excited on the $g_{9/2}$ IAR, the 5492 4^- state on the $d_{5/2}$, $s_{1/2}$ IARs; the energy difference is $\delta E_x = 1.3$ keV (Table III).

Figures 5 and 6 show spectra for ^{208}Pb(p,p') taken on the $g_{9/2}, i_{11/2}, d_{5/2}, s_{1/2}$ IARs in ^{209}Bi. They cover the region $3.9 < E_x < 4.7$ MeV. The doublets at $E_x = 3.96$, $E_x = 4.05$, $E_x = 4.26$, $E_x = 4.70$ MeV are fully resolved. For convenience, the 2^+, 4^+, 6^+, 8^+ yrast states are marked; they are strongly excited by the direct-(p,p') reaction.

The multiplets $g_{9/2}f_{5/2}$, $g_{9/2}p_{3/2}$, $i_{11/2}p_{1/2}$, $i_{11/2}f_{5/2}$, $h_{9/2}s_{1/2}$, $h_{9/2}d_{3/2}$ are identified by the corresponding states with the dominant strength (Table I). The 3708 5^- member of the $h_{9/2}s_{1/2}$ multiplet, and the 4937 3^-, 4919 8^- members of the $i_{11/2}f_{5/2}$ multiplet are outside the shown spectra. The parabolic shape of the multiplet splitting [21] is obvious.

Figures 7–10 show two spectra for ^{208}Pb(p,p') taken near the $g_{7/2}$ IAR in ^{209}Bi under the same conditions covering excitation energies from 4.5 to 6.3 MeV. (A single spectrum taken with the Q3D magnetic spectrograph covers a range of $\Delta E_x \approx 1.0(E_p - E_x^0)$ around a chosen excitation energy E_x^0, where E_p is the incident proton energy.) The number of counts for peaks in the overlapping region is the same within

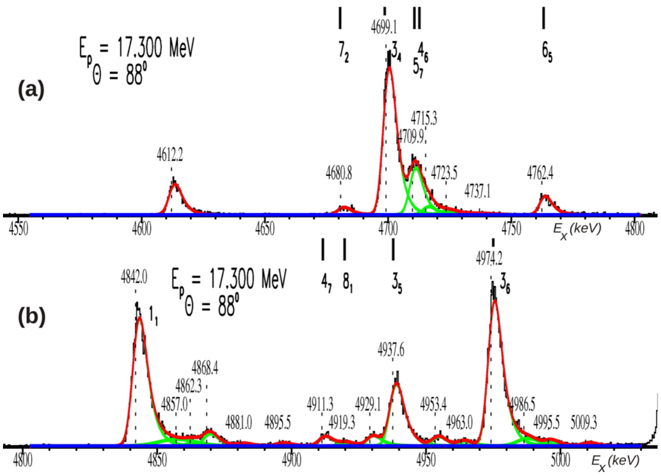

FIG. 7. (Color online) Excerpts of spectra from ^{208}Pb(p,p') near the $g_{7/2}, d_{3/2}$ IARs in ^{209}Bi ($E^{\rm res} = 17.430, 17.476$ MeV, respectively [5]) taken consecutively (a) for $4.55 < E_x < 4.80$ MeV and (b) for $4.80 < E_x < 5.03$ MeV; in Fig. 8 for $5.02 < E_x < 5.46$ MeV, in Fig. 9 for $5.46 < E_x < 5.85$ MeV, and in Fig. 10 for $5.85 < E_x < 6.29$ MeV. For details see Sec. III B.

1%. Since the run time was the same (30 minutes) it proves the high stability of the proton beam from the accelerator—indeed for many hours.

The spectra cover all negative parity states in the region $4.55 < E_x < 6.19$ MeV as discussed in this paper. Each state with negative parity is identified by spin and order number (I_M [Eq. (2)], see Table I). Most other levels correspond to positive parity states; some levels are satellites from L electrons (see Sec. III A).

In contrast to many other (more than 300) ^{208}Pb(p,p') spectra covering energies of scattered protons $7 < E_{p'} < 14$ MeV, no contamination line from light nuclei (^{12}C, ^{14}N, ^{16}O, ^{40}Ar) is present in Figs. 7–10.

Table V lists spectra shown in Figs. 3–10 and previous studies of the ^{208}Pb(p,p') reaction covering the range of excitation energies $2.5 < E_x < 6.5$ MeV with correspondence to the incident proton energy and an IAR, and the chosen scattering angle. Table VI lists spectra shown in previous

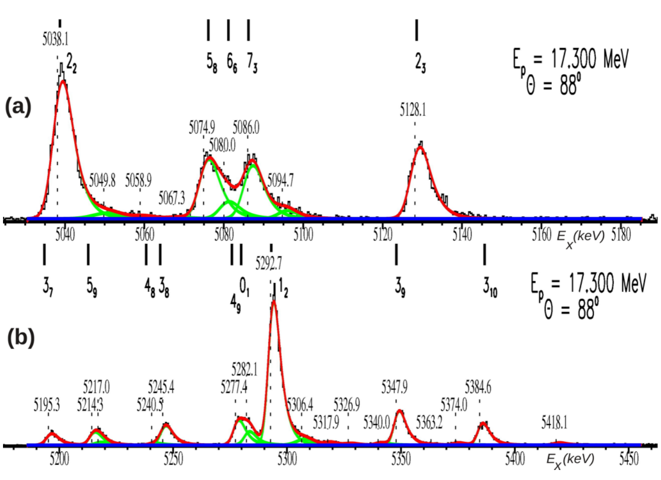

FIG. 8. (Color online) Continuation of Fig. 7, (a) for $5.02 < E_x < 5.19$ MeV and (b) for $5.19 < E_x < 5.46$ MeV.

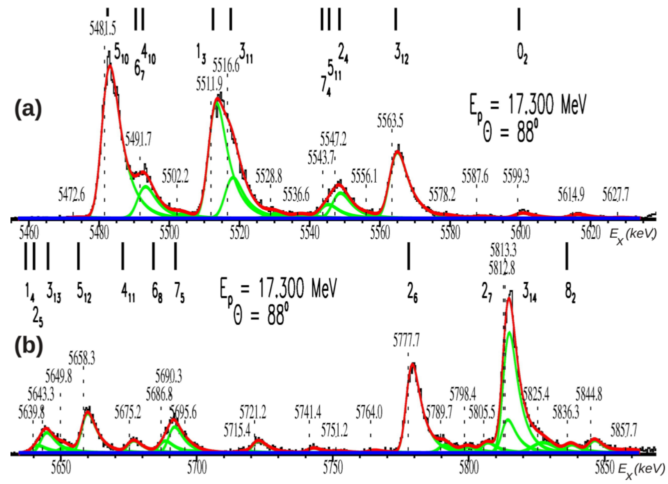

FIG. 9. (Color online) Continuation of Figs. 7–8, (a) for $5.46 < E_x < 5.63$ MeV and (b) for $5.63 < E_x < 5.86$ MeV. The doublet 5812 2_7^-, 5813 3_{13}^- is fitted by assuming a distance of 0.5 keV [20].

studies for the ^{207}Pb(d,p) reaction covering the range $4.6 < E_x < 6.2$ MeV.

C. Poorly resolved 1-keV and 2-keV doublets

Tables III and IV show data on doublets of states with distances of about 0.5–2.0 keV discussed in the following.

In addition, we mention the 3.96 and 4.26 MeV doublets; in Fig. 5 these doublets are fully resolved in the ^{208}Pb(p,p') reaction. The 3947 4_2^- state was already resolved in the experiment on the $g_{9/2}$ IAR by Richard *et al.* [7].

The 5193 5^+, 5195 3^-, 5196 7^+ doublet. NDS2007 suggests the 5.19 MeV level to contain three states: the 5193 5^+, 5196 7^+ states with dominant $h_{9/2}h_{11/2}$ components [10,12,13], and in addition the 5195 state with negative parity; it is assigned the spin of 3^- (Sec. IV C).

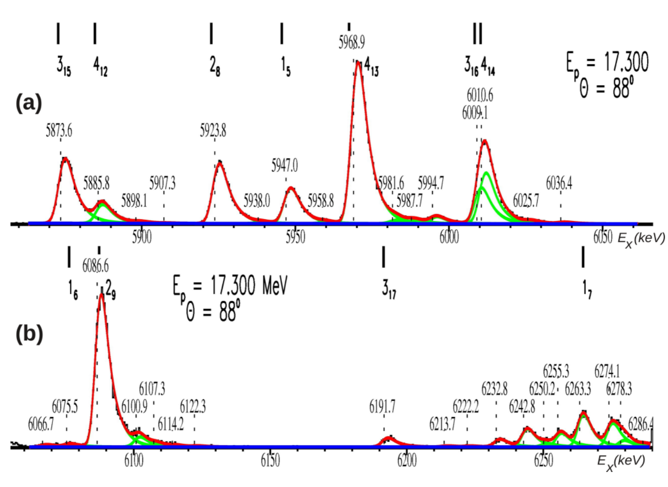

FIG. 10. (Color online) Continuation of Figs. 7–9, (a) for $5.86 < E_x < 6.05$ MeV and (b) for $6.05 < E_x < 6.29$ MeV. Except for the 1_6^-, 2_9^-, 3_{17}^- states, no negative parity state in the region $6.02 < E_x < 6.21$ MeV is known. The gap corresponds to the predicted gap $5922 \leqslant E_x^{\rm SSM} \leqslant 6361$ keV for spins 4^- - 7^- [13].

TABLE IV. Complement of Table III: Mean cross sections of ^{207}Pb(d,p) and of ^{208}Pb(p,p') near all known IARs in ^{209}Bi. The (reinterpreted) spectroscopic factor yielding $[c_{LJ,lj}]^2 = \frac{2}{2I+1} G_{LJ}$ from Ref. [32] is included.

Level		$\sigma^{(p,p')\mathrm{a}}$						$\sigma^{(d,p)\mathrm{b}}$	G_{LJ}	LJ
IAR: E_p (MeV) =		$g_{9/2}$ 14.92	$i_{11/2}$ 15.72	$(j_{15/2})$ 16.38	$d_{5/2}$ 16.45	$s_{1/2}$ 16.96	$g_{7/2}{}^{\mathrm{c}}$ 17.43	Eq. (16)	[32]	[32]
$\tilde{E}_x$	I^π_M	(μb/sr)	(μb/sr)	(μb/sr)	(μb/sr)	(μb/sr)	(μb/sr)	(μb/sr)	$\times 1000$	
4911	4^-_7	2.0 ± 0.5	2 ± 1	2 ± 1	$3 \pm 1^{\mathrm{d}}$	<2	2 ± 1	7 ± 2	$5 + 5$	$g_{9/2} + g_{7/2}{}^{\mathrm{e}}$
4937	3^-_5	4 ± 1	<1	15 ± 2	15 ± 2	10 ± 3	<5	35 ± 5	$32 + 25$	$d_{5/2} + g_{7/2}$
4953	3^+_1	0.8 ± 0.4	2 ± 1	1.5 ± 0.5	$1.0 \pm 0.5^{\mathrm{d}}$	1.5 ± 0.5	<2	<0.5		
5193	5^+_2	0.8 ± 0.4	2 ± 1	3 ± 1	<1	4 ± 2	4 ± 2	<2.0		
5195	3^-_7	1.0 ± 0.3	$3 \pm 1^{\mathrm{d}}$	5 ± 1	$5 \pm 2^{\mathrm{d}}$	3 ± 1	3 ± 1	20 ± 5	38	$g_{7/2}$ f
5196	7^+_3	1.0 ± 0.5	2 ± 1	5 ± 1	5 ± 2	<3	6 ± 3	<10		
5213	6^+_3	10 ± 3	<1	2 ± 1	<3	<3	<3	<0.5		
5214	5^-_9	12 ± 2	<1	1.0 ± 0.5	$12 \pm 4^{\mathrm{d}}$	8 ± 5	10 ± 5	50 ± 5	30	$g_{9/2}{}^{\mathrm{e}}$
5216	4^+_2	2 ± 1	<2	$2 \pm 1^{\mathrm{d}}$	<2	<2	2 ± 1	<0.5		
5235	11^+_1	<2	<1	1.0 ± 0.5	<1	<1	<1	<0.5		
5383	4^+	<1	2 ± 1	5 ± 3	<5	<5	<3	<0.5		
5385	3^-_{10}	5 ± 3	5 ± 3	30 ± 5	50 ± 10	15 ± 5	5 ± 3	140 ± 5	155	$d_{5/2}$
5490	6^-_7	4 ± 1	5 ± 2	<5	<5	<2	<2	<0.5		
5492	4^-_{10}	3 ± 1	5 ± 2	70 ± 10	120 ± 10	30 ± 10	10 ± 5	35 ± 5	66	$g_{7/2}$
5640	1^-_4	1.5 ± 0.5	<1	<1	<1	2 ± 1	<1	20 ± 5		g
5642	2^+	$1.0 \pm 0.5^{\mathrm{d}}$	<2	$15 \pm 6^{\mathrm{d}}$	$<20^{\mathrm{d}}$	10 ± 5	10 ± 5	<0.5		
5643	2^-_5	4 ± 2	2 ± 1	$20 \pm 5^{\mathrm{d}}$	25 ± 5	5 ± 3	3 ± 2	<0.5		
5648	3^-_{13}	<1	<1	15 ± 10	20 ± 5	<1	<1	8 ± 5		g
5649	9^+_4	<1	<1	8 ± 4	5 ± 3	<5	<3	<2.0		
5675	4^-_{11}	1.5 ± 0.5	$1.5 \pm 0.5^{\mathrm{d}}$	$4 \pm 3^{\mathrm{d}}$	$5 \pm 2^{\mathrm{d}}$	3 ± 2	<3	20 ± 5		g

[a] The mean cross section is evaluated for $80^\circ \lesssim \Theta < 115^\circ$ [Eq. (13)].
[b] The mean cross section is evaluated from data taken in 2004 for $\Theta = 20^\circ, 25^\circ, 30^\circ$ [15].
[c] The $d_{3/2}$ IAR with $E^{\mathrm{res}} = 17.48$ MeV and $E^{\mathrm{tot}} = 280$ keV [5] contributes too.
[d] Steep raise below $\Theta \approx 50^\circ$.
[e] Reinterpreted ^{207}Pb(d,p) data (Sec. III D).
[f] Recent experiments indicate a $j_{15/2}$ component.
[g] L value not determined.

The 5.19 MeV doublet was not resolved in the work of Valnion *et al.* but 0.038 $g_{7/2}p_{1/2}$ strength was determined indicating the presence of a negative parity state [32]. The ^{207}Pb(d,p) data from 2004 [15] resolve the doublet indicating the middle state carries most of the observed cross section (Tables III and IV).

The 5213 6^+, 5214 5^-, 5216 4^+ doublet. The 5213 6^+, 5216 4^+ states are discussed in Ref. [13]. The 5214 state is assigned the spin of 5^- (Sec. IV C). In relation to the neighboring 5.19 MeV peak, the 5.21 MeV level is more strongly excited on the $g_{9/2}$ IAR (Fig. 4). Large $h_{9/2}h_{11/2}$ components were observed in the unresolved level [10,12], but a $h_{9/2}d_{5/2}$ admixture cannot be excluded.

Valnion *et al.* [32] deduced a $d_{5/2}p_{1/2}$ admixture for the 5214 state. Yet the angular distribution of the analysis power can be interpreted by $g_{9/2}p_{1/2}$ as well; a $i_{11/2}p_{1/2}$ or $g_{7/2}p_{1/2}$ admixture is excluded, however. Section IV C shows the 5214 state to have the spin of 5^-. The 5213 6^+, 5216 4^+ states are not observed by the ^{207}Pb(d,p) reaction (Table IV).

The 5383 4^+, 5385 3^- states. Spectra taken near the $j_{15/2}$, $d_{5/2}$ IAR reveal a close neighbor to the 5385 3^- state (Fig. 3). The 5383 state with spins 3^+, 4^+, 5^+ suggested by NDS2007 is thus confirmed (Tables III and IV); in Sec. IV C assignments of spin 3^+ and 5^+ are excluded.

The angular distribution of the 5383, 5385 doublet taken for the ^{209}Bi$(d,{}^3$He$)$ reaction is clearly fitted by $L = 2$ (see Fig. 4 of Ref. [10]; apparently the entry in Table 1 is misplaced.)

The 5490 6^-, 5492 4^- doublet. The 5490 6^- is excited on the $g_{9/2}$ IAR while the 5492 4^- state is excited on the $d_{5/2}$ IAR. The distance between the two states is 1.3 ± 0.3 keV (Table III) in congruence with the suggested value of 1.2 ± 0.1 keV [14].

A large $h_{9/2}d_{5/2}$ component was observed in the unresolved doublet [10,12] (Sec. II C 3). A considerable $g_{7/2}p_{1/2}$ fraction was determined by the ^{207}Pb(d,p) reaction with polarized deuterons [32] (Table IV).

Luckily, the 5492 4^- state has the higher excitation energy, therefore in most spectra taken on the $d_{5/2}$ IAR the 5490 6^- state can be shown to be not excited at all with the resolution of 1.5 keV HWHM on the low excitation energy side [13]. The valley between the 5482 and the 5492 levels is often five times lower than the adjacent peaks (Figs. 3 and 4).

On the $g_{9/2}$ IAR in reverse, the 5490 6^- state is more strongly excited than the 5492 4^- state; in Fig. 4 (taken with a thin target, and hence higher resolution) only the former state shows up. The 5490 state is not observed by the ^{207}Pb(d,p) reaction.

The 5.64 MeV doublet. The 5.64 MeV doublet contains five states within 10 keV. In the whole region $2.6 < E_x < 6.2$ MeV, it is the densest ensemble of states. The two doublets at $E_x =$ 5.19 and 5.21 MeV with six states cover already 30 keV and the mean spacing is even 10 keV.

The five states are grouped into two doublets separated by 5 keV: namely the 5640 1^-, 5642 2^+, 5643 2^- states in the first doublet, and the 5648 3^- state and the 5649 state (assigned the spin of 9^+ [13]) in the second doublet. The distances between the states in the first doublet are 2.5 and 0.8 keV, and 0.5 keV in the second doublet (Table III).

The excitation functions and the angular distributions of the five members are extremely different. Therefore many spectra were already shown, see Table V.

The 5640 state is mainly excited on the $g_{9/2}$ IAR and weakly on the $s_{1/2}$ IAR, and the 5643 state strongly on the $d_{5/2}$ IAR. The 5648 3^-, 5649 9^+ states are excited on the $d_{5/2}$, $j_{15/2}$ IARs with about equal mean cross sections; even the angular distributions are similar. The 5648 3^- state is excited on the $g_{9/2}$ IAR too [13].

The 5642 state is assigned the spin of 2^+, a suggested spin 1^+ or 1^- [14] is excluded. The excitation function of the 5642 state for energies $17.3 < E_p < 18.1$ MeV (beyond the $s_{1/2}$ IAR) is smooth, indicating the excitation by the direct-(p,p') reaction.

The 5640 1^-, 5642 2^+, 5643 2^- states are not well resolved by the ^{208}Pb$(p,p'\gamma)$ [6,40] and ^{207}Pb$(d,p\gamma)$ experiments [6,12,40]. The excitation of the 5643 2^- state on the $d_{5/2}$ IAR is confirmed by the 5.63 MeV γ-ray reported in the ^{208}Pb$(p,p'\gamma)$ experiment by Cramers *et al.* [6]. Radermacher *et al.* [40] state an additional excitation on the $s_{1/2}$ IAR. Both the ^{208}Pb$(p,p'\gamma)$ [40] and the ^{207}Pb$(d,p\gamma)$ [12] experiment yield an uncertainty of 0.5 keV for the 5641 keV γ transition. The ^{208}Pb$(n,n'\gamma)$ experiment shows both the 5640 1^- and the 5642 2^+ state to deexcite to the ground state.

Large $h_{9/2}d_{5/2}$, $h_{9/2}h_{11/2}$ components were observed by the ^{209}Bi$(d,{}^3$He$)$, ^{209}Bi$(t,\alpha\gamma)$ reactions in the two unresolved doublets and the following levels up to $E_x = 5.72$ MeV—comprising eleven states within 75 keV at a resolution of 15 keV [10–12]; see Secs. IV A, IV C, and IV D 8.

D. States weakly excited by the ^{208}Pb(p,p') and the ^{207}Pb(d,p) reactions

Here, we discuss data not presented previously [13,15–20].

The 4911 4^- state is excited on the $d_{5/2}$ IAR somewhat more strongly than on other IARs, but the cross section is still weak (Table IV, Fig. 7).

Valnion *et al.* [32] deduced from the ^{207}Pb(d,p) reaction a spectroscopic factor $G_{j_{15/2}} = 440$. However, the angular distribution both of the differential cross section and of the analyzing power may be interpreted equally well by a mixture of nearly equal parts of the configurations $g_{9/2}p_{1/2}$ and $g_{7/2}p_{1/2}$ with 0.1% strength each (Table IV).

The 4937 3^- state is excited on the $d_{5/2}$ IAR in an enhanced manner (Fig. 7) and weakly by the ^{207}Pb(d,p) reaction (Table IV). Valnion *et al.* [32] deduced about equal fractions of $d_{5/2}p_{1/2}$ and $g_{7/2}p_{1/2}$, yielding strengths 0.9% and 0.7%, respectively. A weak $h_{9/2}d_{3/2}$ component was observed [10,12].

The 4953 3^+ state has a vanishing ^{207}Pb(d,p) cross section and the direct-(p,p') cross section is low (Table IV, Fig. 7). It is not excited by the ^{209}Bi$(d,{}^3$He$)$ reaction [10,12].

The 5235 11^+ state is weakly excited on the $g_{9/2}$ IAR. On the $j_{15/2}$ IAR, a weak resonance is observed (Table IV). It is not observed by the ^{208}Pb(p,p') reaction at higher proton energies. The ^{207}Pb(d,p) cross section is vanishingly small.

The 5675 4^- state. The 5675 4^- state has a low cross section on all IARs (Fig. 8), but for the ^{207}Pb(d,p) a considerable cross section is observed (Table IV) corresponding to about 0.5% $g_{7/2}p_{1/2}$ strength [32].

The 5675 4^- state is strongly excited by the ^{209}Bi$(t,\alpha\gamma)$ reaction [12]. The distance to the next neighboring states with at distances of 11 and 17 keV allows us to prove the 5675 state to be the most strongly excited in the ensemble of eleven states at $5.64 < E_x < 5.72$ MeV, albeit the resolution in the ^{209}Bi$(d,{}^3$He$)$ reaction was only about 12 keV [10,11].

E. Data from other experiments

Recent ^{208}Pb(γ,γ') [41,42] and ^{208}Pb$(\vec{p},\vec{p})$ experiments [43,44] studied the 1^- states in ^{208}Pb at $E_x \lesssim 7.5$ MeV. They do not observe the 5640 1^- state (Sec. III C).

Results from experiments on the ^{208}Pb$(p,p'\gamma)$ [6,40], the ^{207}Pb$(d,p\gamma)$ [12,40], and the ^{209}Bi$(t,\alpha\gamma)$ [12] reactions are discussed in Sec. III C.

Data from other experiments are considered, but not discussed in detail. We rely on the evaluation by NDS2007.

The ^{208}Pb(α,α') reaction excites only natural parity states. Apparent exceptions for the levels near the 5037 2^-_2, 5836 8^-_2 states may be explained by unresolved neighbors which are not yet identified.

The L values determined from the ^{208}Pb(p,p') reaction at $E_p = 35$ MeV by Wagner *et al.* [45] generally agree with the given spin assignments; in some cases, they deviate by one unit. Several doublets which are now disentangled were already recognized by Wagner *et al.*

Data from the ^{208}Pb$(n,n'\gamma)$ reaction are shown in NDS2007, but without information about excitation functions. The uncertainty of the excitation energies for the adopted levels apparently reflect in most cases the systematic error only [39].

IV. DISCUSSION

Table I shows the configurations predicted by the SSM up to $E_x^{\rm SSM} = 6536$ keV. Below $E_x^{\rm SSM} = 6361$ keV each configuration with spins 0^-–8^- can be matched to a certain state by choosing the leading strength c_1^2 shown under column "1. State". For about half of the configurations, a single state contains more than 60% of the total strength.

For many configurations, a second state completes the total strength to more than 80%, often up to more than 90% (column "2. State"). In case more admixtures are known, the admixtures

TABLE V. List of spectra taken for the ^{208}Pb(p,p') reaction. The energy E_p of the incident proton and the scattering angle Θ are given; the nearest IAR in ^{209}Bi is shown. Most spectra are fitted by GASPAN [38]; they are marked by "yes" in column 2.

Range E_x (keV)	Fit	Ref.	E_p (MeV)	IAR	Θ (deg)	E_p (MeV)	IAR	Θ (deg)	E_p (MeV)	IAR	Θ (deg)	E_p (MeV)	IAR	Θ (deg)	E_p (MeV)	IAR	Θ (deg)
2500–7100		[2]	14.95	$g_{9/2}$	90				16.45	$d_{5/2}$	90	17.00	$s_{1/2}$	90	17.40	$g_{7/2}$	90
3895–4005[a]	yes	[22]	14.920	$g_{9/2}$	84												
3910–4240	yes	Fig. 5	14.920	$g_{9/2}$	58	15.720	$i_{11/2}$	115	16.495	$d_{5/2}$	88	16.960	$s_{1/2}$	84			
4240–4770	yes	Fig. 6	14.920	$g_{9/2}$	58	15.720	$i_{11/2}$	115	16.495	$d_{5/2}$	88	16.960	$s_{1/2}$	84			
4475–4570[a]	yes	[22]	14.920	$g_{9/2}$	99												
4550–4800	yes	Fig. 7													17.300	$g_{7/2}$	88
4580–6150[b]		[19]	14.920	$g_{9/2}$	88	15.720	$i_{11/2}$	115	16.495	$d_{5/2}$	88	16.960	$s_{1/2}$	84	17.480	$d_{3/2}$	84
									16.495	$d_{5/2}$	90	16.960	$s_{1/2}$	138			
4670–5000		[15]	14.920	$g_{9/2}$	58												
4678–4722	yes	[22]				15.720	$i_{11/2}$	84									
4800–5030	yes	Fig. 7													17.300	$g_{7/2}$	88
4830–4920	yes	[23]							16.390	$j_{15/2}$	138	16.500	$d_{5/2}$	138			
4835–4935	yes	[13]							16.390	$j_{15/2}$	138	16.500	$d_{5/2}$	138			
4920–5105	yes	[13]							16.260	$j_{15/2}$	138	16.370	$j_{15/2}$	138	16.460	$d_{5/2}$	138
5020–5290		[15]	14.920	$g_{9/2}$	58	15.720	$i_{11/2}$	72	16.495	$d_{5/2}$	54						
5020–5190	yes	Fig. 8													17.300	$g_{7/2}$	88
5020–5440		[32]													22.000	off	50
5180–5510	yes	Fig. 9	14.920	$g_{9/2}$	88	15.720	$j_{15/2}$	81	16.390	$j_{15/2}$	138	16.495	$d_{5/2}$	90			
												16.960	$s_{1/2}$	84	17.610	$g_{7/2}$	84
5185–5290	yes	[15]				15.720	$i_{11/2}$	29	15.720	$i_{11/2}$	66						
5190–5460	yes	Fig. 8													17.300	$g_{7/2}$	88
5300–5700		[13]							16.405	$j_{15/2}$	88						
5400–6030		[52]													22.000	off	40
5460–5570	yes	Fig. 4	14.920	$g_{9/2}$	58				16.495	$d_{5/2}$	90	16.960	$s_{1/2}$	84			
5460–5630	yes	Fig. 9													17.300	$g_{7/2}$	88
5460–6120		[24]	14.920	$g_{9/2}$	88				16.405	$j_{15/2}$	88	16.500	$d_{5/2}$	138			
5560–5660	yes	[22]							16.355	$j_{15/2}$	48	16.495	$d_{5/2}$	75	16.960	$s_{1/2}$	78
5610–5705	yes	[24]	14.920	$g_{9/2}$	88							16.405	$j_{15/2}$	88			
5610–5710	yes	[13]				16.260	$j_{15/2}$	138	16.405	$j_{15/2}$	42	16.405	$j_{15/2}$	88	16.500	$d_{5/2}$	138
5630–5710	yes	[17]	14.920	$g_{9/2}$	25, 42	14.920	$g_{9/2}$	58, 88	15.720	$i_{11/2}$	81	16.495	$d_{5/2}$	88	16.960	$s_{1/2}$	88
5630–5860	yes	Fig. 9													17.300	$g_{7/2}$	88
5760–5920	yes	[17]	14.920	$g_{9/2}$	25	15.070	$g_{9/2}$	42									
5700–6100		[13]							16.405	$j_{15/2}$	88	16.630	$d_{5/2}$	88			
5860–6050	yes	Fig. 10													17.300	$g_{7/2}$	88
5880–6005	yes	[13]							16.405	$j_{15/2}$	88	16.495	$d_{5/2}$	88	16.580	$d_{5/2}$	88
5960–6030	yes	[20]							16.495	$d_{5/2}$	48				17.300	$g_{7/2}$	138
6050–6290	yes	Fig. 10													17.300	$g_{7/2}$	88
6060–6230	yes	[18]							16.500	$d_{5/2}$	138	16.960	$s_{1/2}$	138	17.300	$g_{7/2}$	88
6180–6500	yes	[18]							16.495	$d_{5/2}$	48	16.960	$s_{1/2}$	48	17.300	$g_{7/2}$	88

[a]The line shape of peaks distorted by the knockout of L,M electrons is studied [22].
[b]The spectra are divided up into two parts taken under different conditions.

in further states are mostly less than 10%. For this reason, only the two largest fractions are shown for each configuration. (For nine states in reverse, three configurations are shown.)

The spin weighted sum rules S_{LJlj} for each configuration $LJlj$ [Eq. (10)] yield a mean value close to 90% (Table I). Including the known strength in more states improves the yield.

The spin weighted centroid energy $\overline{E_x^{\rm cnt}}$ for each configuration $LJlj$ [Eq. (19)] is close to the SSM energy $E_x^{\rm SSM}$ [13] (Table I). The difference is less than 50 keV with few exceptions; here the major strengths are determined with large uncertainties or larger fractions are not yet located (Sec. IV F).

In the following, positive parity states are discussed only if (i) they are a member of doublet with a negative parity state closer than about 2 keV and (ii) the excitation energy is below $E_x = 5.85$ MeV, or if (iii) NDS2007 either suggests negative parity or no parity.

A. Confirmed spin assignments for negative parity states

When the first experiments on inelastic proton scattering via IAR were performed [1–9], little was known about the

TABLE VI. List of spectra taken for the ^{207}Pb(d,p) reaction. The energy E_d of the incident deuteron and the scattering angle Θ are given. Most spectra are fitted by GASPAN [38]; they are marked by "yes" in col. 2.

^{207}Pb(d,p)				
Range(E_x) (keV)	Fit	Ref.	E_d (MeV)	Θ (deg)
4650–6150		[19]	22.0	20
4900–6050		[32]	22.0	37.5
4955–5085	yes	[13]	22.0	30
5020–5430		[32]	22.0	50
5230–5360	yes	[16]	22.0	30
5400–6030		[52]	20.0	40
5540–5650	yes	[16]	22.0	25

states in ^{208}Pb. Alone, the comparison of the volume of the Nuclear Data Sheets of 1971 [46] with those of 2007 [14] reveals the progress in knowledge on ^{208}Pb; the former volume has eleven pages on data related to the doubly magic nucleus ^{208}Pb compared to one hundred pages now.

Among the lowest twenty negative parity states predicted by the SSM, only about half of them had spin assignments before 1971 which are now accepted.

The first analysis of the lowest twenty negative parity states done in 1973 was essentially based on data for the ^{208}Pb(p,p') reaction via the $g_{9/2}$ and $d_{5/2}$ IARs [9]. A few assignments and one state identification were erroneous [29].

A long ^{207}Pb(d,p) exposure with the Buechner magnetic spectrograph at $\Theta = 130^\circ$ [15] was important. For the proton particle-hole configurations, the analysis was based on the ^{209}Bi(t,α) experiment with a resolution of 50 keV [47], on the ^{209}Bi$(d,{}^3$He) experiment with a resolution of 60–75 keV [48], and unpublished data from a ^{209}Bi$(d,{}^3$He) experiment with a resolution of 70 keV [49].

The ^{209}Bi$(d,{}^3$He) experiment done in 1981 with a mean resolution of 15 keV [10] was decisive for the disentanglement of the $h_{9/2}s_{1/2}$ doublet at $E_x = 3.95$ MeV. The spin assignments of the lowest twenty negative parity states below $E_x = 4.6$ MeV could be settled; they are now accepted [14]. The dominant particle-hole configurations are determined with good precision [31].

1. Spin assignments from NDS2007 below $E_x = 6.1$ MeV

When NDS2007 appeared [14], two thirds of the negative parity states below $E_x = 6.1$ MeV had spin assignments which are now confirmed. Several suggested identifications and spin assignments are now verified.

Except for the 2615 3^- yrast state, the negative parity states below $E_x = 4.5$ MeV have the dominant configurations $g_{9/2}p_{1/2}$, $g_{9/2}f_{5/2}$, $g_{9/2}p_{3/2}$, $h_{9/2}s_{1/2}$, $h_{9/2}d_{3/2}$, $i_{11/2}p_{1/2}$ [29,31]. Figures 5 and 6 identify these states in ^{208}Pb(p,p') spectra. (Some states are below $E_x = 3.9$ MeV.)

Ordered by the spin, below $E_x = 4.5$ MeV there are the 4230 2^-_1 state, the 2615 3^-_1, 4051 3^-_2, 4255 3^-_3 states, the 3475 4^-_1, 3947 4^-_2, 3995 4^-_3, 4262 4^-_4, 4359 4^-_5 states, the 3198 5^-_1, 3961 5^-_2, 3708 5^-_3, 4125 5^-_4, 4180 5^-_5, 4297 5^-_6 states, the 3920 6^-_1, 4206 6^-_2, 4383 6^-_3, 4481 6^-_4 states, and the 4037 7^-_1 state.

Above $E_x = 4.5$ MeV there are the 5280 0^-_1, 5599 0^-_2, 4841 1^-_1, 5292 1^-_2, 5512 1^-_3, 5640 1^-_4, 5947 1^-_5, 5548 2^-_4, 5924 2^-_8, 4698 3^-_4, 4937 3^-_5, 4974 3^-_6, 5245 3^-_8, 5347 3^-_9, 5385 3^-_{10}, 5517 3^-_{11}, 5564 3^-_{12}, 5813 3^-_{14}, 5874 3^-_{15}, 6011 3^-_{16}, 4911 4^-_7, 5969 4^-_{13}, 5482 5^-_{10}, 5659 5^-_{12}, and 5543 7^-_4 states.

As shown in Sec. IV D 3, the 4841 1^- and 2615 3^- yrast states are not described by the SSM configurations below $E_x =$ 6361 keV.

2. Spin assignments since NDS2007

Since the appearance of ND2007 several new states were identified and many spins were either newly assigned or suggested spins were confirmed [13,15–20]. The negative parity states with new or confirmed spin assignments are underlined in Table I. New and confirmed assignments by this work are shown in Table III. The suggested assignment of the spin 5^- to the 5545 state [12] is accepted.

The spins of the 4680, 4709, 4712, 4762, 4919, 5080, 5085, 5239, 5276 states from the study of the proton decay of the $i_{11/2}$ IAR [15] were already included in NDS2007. Similarly, the preliminary assignments of spins 6^-, 7^-, 8^- to the 5686, 5694, 5836 states from the study of the proton decay of the $g_{9/2}$ IAR mentioned in Ref. [15] were already included; the angular distributions proving the assignments were shown later [17].

The proton decay of the $j_{15/2}$ IAR revealed many positive parity states [13] which are not extensively discussed here. Several negative parity states were confirmed or identified, but no definitive spin was assigned.

The 5038, 5127, 5778, 6087, 6420, 6552, 6657 states were determined to have the spin of 2^- in studying the proton decay of the $s_{1/2}$ IAR [18]; see also Fig. 1. The spin of both the 5886 and the 6012 state was determined as 4^- by the study of the proton decay of the $d_{5/2}$ IAR; the 5812 2^- state was newly identified [20],

The spins of the 5195, 5490, 5492, 5643, 5648 states are newly assigned; the assignments of spin 5^-, 4^- to the 5214, 5675 states, respectively, are confirmed; the assignments of spin 4^-, 1^- to the 4911, 5640 states, respectively, are verified (Table III, Sec. IV C). In addition, the parity of 4953 state is shown to be positive (with the spin of 3^+); the assignment of spin 11^+ to the 5235 state is confirmed; and the 5383, 5642 states are assigned the spins of 4^+, 2^+, respectively.

B. The two major fractions of configurations

In the following, the two major configuration fractions in the states shown in Table I are discussed.

States with dominant configurations $i_{11/2}f_{5/2}$, $i_{11/2}p_{3/2}$. The $i_{11/2}f_{5/2}$ multiplet with the 4712 4^-_6, 4709 5^-_7, 4762 6^-_5, 4680 7^-_2, 4919 8^-_1 states contain less than 10% admixture of other configurations [15]. For the 3^- strength see Sec. IV D 7. The 4709 5^-_7 has some percent strength admixtures of $g_{9/2}p_{1/2}$, $i_{11/2}p_{1/2}$ as observed by the excitation in the ^{207}Pb(d,p) reaction; it also contains a considerable $h_{9/2}d_{5/2}$ admixture [12]. The 4762 6^-_5 has a weak $i_{11/2}p_{1/2}$ admixture.

The $i_{11/2}p_{3/2}$ multiplet with the 5075 5^-_8, 5080 6^-_6, 5085 7^-_3 states contain less than 10% admixture of other configurations [15]. The 4^- strength is split with the ratio 1 : 9 between the 5239, 5276 states; the undetectable configuration $f_{7/2}d_{3/2}$ contributes mainly the remaining strength. The excitation in the ^{207}Pb(d,p) reaction reveals a few percent admixture of $g_{7/2}p_{1/2}$ in the 5276 state which also shows up as a resonant enhancement on the $g_{7/2}$ IAR.

States with dominant configuration $d_{5/2}p_{1/2}$. The 5038 2^-_2 [18], 5127 2^-_3 [18], and the 4698 3^-_4, 4974 3^-_6, 5245 3^-_8 states contain the major fractions of the $d_{5/2}p_{1/2}$ strength; weak fractions are found in the 4230 2^-_1, 4255 3^-_3, states [15,20,32,36].

States with dominant configuration $g_{9/2}f_{7/2}$. The 5659 5^-_{12}, 5686 6^-_8, 5694 7^-_5, 5836 8^-_2 states contain 70%, 90%, 90%, 98% of the $g_{9/2}f_{7/2}$ strength, respectively [17]. For the 1^-, 2^-, 3^-, 4^- strengths see Sec. IV C.

States with dominant configuration $d_{5/2}p_{3/2}$. The 5947 1^-_5, 6264 1^-_7, 6314 1^-_9, 5778 2^-_6, 5812 2^-_7, 5924 2^-_8, 5813 3^-_{14}, 5874 3^-_{15}, 6011 3^-_{16}, 5886 4^-_{11}, 5969 4^-_{13}, 6012 4^-_{14}, states contain 17%, 26%, 51%, 33%, 54%, 7%, 50%, 33%, 16%, 29%, 7%, 68%, of the $d_{5/2}p_{3/2}$ strength, respectively; the uncertainties are about 5%, but 13% and 25% for the 6264 1^-_7, 6314 1^-_9 states [20]. The 5292 1^-_2, 5512 1^-_3 states certainly contain also a few percent $d_{5/2}p_{3/2}$ strength besides strong $d_{5/2}f_{5/2}$ components.

The 5947 1^-_5 state contains 90% of the $d_{3/2}p_{1/2}$ strength; the 6264 1^-_7, 6314 1^-_9 states about 5% $s_{1/2}p_{1/2}$ strength with little $d_{3/2}p_{1/2}$ admixture [32].

The 5813 3^-_{14}, 6011 3^-_{16} states have 12%, 30% $g_{7/2}p_{1/2}$ admixtures and the 5874 3^-_{15} state the major $g_{7/2}p_{1/2}$ fraction (60%) [32].

The 5969 4^-_{13} state contains the major $g_{7/2}p_{1/2}$ fraction and the 5886 4^-_{11} state 20% $g_{7/2}p_{1/2}$ admixture [32]. The 6012 4^-_{14} state is not excited by the ^{207}Pb(d,p) reaction [20], hence a $g_{9/2}p_{1/2}$ or $g_{7/2}p_{1/2}$ admixture is less than 1%.

The 6011 3^-_{16} state is strongly excited on the $g_{7/2}$ IAR [5] suggesting a strong $g_{7/2}f_{5/2}$ component; we assume 40%–70% (Table I).

The 0^-, 1^- states with dominant configurations $s_{1/2}p_{1/2}$, $d_{5/2}f_{5/2}$. The two 0^- states share the $s_{1/2}p_{1/2}$ and $d_{5/2}f_{5/2}$ strength completely; any other configuration contributes less than 3% [16].

The 5292 1^-_2 and 5512 1^-_3 states share most of the $s_{1/2}p_{1/2}$ and $d_{5/2}f_{5/2}$ strength. A 10% $d_{3/2}p_{1/2}$ admixture in the 5512 1^-_3 state was determined by ^{207}Pb(d,p) [32]. The distribution of the $d_{5/2}f_{5/2}$ strength cannot be determined from the ^{208}Pb(p,p') reaction because of the strong interference of the $d_{5/2}$ with the neighboring $s_{1/2}$ IAR. (The angular distribution on the $s_{1/2}$ IAR is not isotropic as expected.)

The 2^-, 3^-, 4^-, 5^- states with dominant configuration $d_{5/2}f_{5/2}$. The 5347 state contains the major $d_{5/2}f_{5/2}$ strength for the spin of 3^-, the 5482, 5658 states for 5^-. The dominant strength for the spins 2^- and 4^- is located in the 5643 and 5492 states (Sec. IV C).

States with dominant configuration $h_{9/2}d_{5/2}$. The ^{209}Bi$(d,{}^3$He), ^{209}Bi$(t,\alpha\gamma)$ reactions had been extensively studied [10,12]. Yet, the *"correspondence of the levels in the region* $5.6 < E_x < 5.8$ *MeV is unclear"* as Schramm *et al.* [12] themselves state. Sec. IV C resolves the puzzle.

Positive parity states. Positive parity states had been extensively studied while investigating the proton decay of the intruder IAR $j_{15/2}$ [13]. In this paper, we restrict the discussion mainly to negative parity states; yet of course, several doublets have members of different parity (Tables III and IV, Secs. IV C and IV D 10).

C. New spin and parity assignments and confirmed suggestions

We limit the discussion to states below $E_x \approx 5.85$ MeV.

The 4911 4^- state with dominant configuration $f_{7/2}s_{1/2}$. The schematic shell model [13] (SSM) predicts fourteen states with the spin of 4^- at $E_x^{\rm SSM} < 6487$ keV. The composition of the five lowest states had been determined in 1973 [29], now with correct spin assignments [31]. The next state ($M = 6$) consists almost entirely of the $i_{11/2}f_{5/2}$ configuration [15]. The 8th and 9th states share the $i_{11/2}p_{3/2}$ and $f_{7/2}d_{3/2}$ strength with a ratio 9 : 1, but in reverse order [15]. The three highest states below $E_x = 6.1$ MeV ($M = 12,13,14$) share the complete $d_{5/2}p_{3/2}$ and $g_{7/2}p_{1/2}$ strength [20]. The $g_{9/2}f_{7/2}$ and $h_{9/2}d_{5/2}$ strength is shared by the 10th and 11th states. Two 4^- states with the major $f_{7/2}s_{1/2}$ and $d_{5/2}f_{5/2}$ strength are missing from the prediction.

The 4911 state is assigned the spin of 4^- [14]. The assignment of a dominant $f_{7/2}s_{1/2}$ strength is supported by all data. The largest admixtures of neutron particle-hole configurations are found for $d_{5/2}p_{3/2}$ with 1% strength from the ^{208}Pb(p,p') reaction and 0.1% $g_{9/2}p_{1/2}$ and 0.1% $g_{7/2}p_{1/2}$ from the ^{207}Pb(d,p) reaction (Sec. III D).

The 5675 4^- state with dominant configuration $h_{9/2}d_{5/2}$. The reanalysis of ^{209}Bi$(d,{}^3$He) data [11] clearly resolves the 5675 4^- state from the ensemble of states in a distance of 16 keV below and more than 11 keV above. The next states are the 5658 5^- and the 5686 6^- states. No other state is observed in the region $5.659 < E_x < 5.686$ MeV both by the ^{208}Pb(p,p') and the ^{207}Pb(d,p) reactions. The two ensembles below and above, however, contain both negative and positive parity states excited with $l = 2$ and $l = 5$ components in the ^{209}Bi$(d,{}^3$He) reaction.

The proposed assignment of the spin of 4^- to the 5675 state from the ^{209}Bi$(t,\alpha\gamma)$ experiment [12] is acknowledged; the $h_{9/2}d_{5/2}$ strength is determined to be nearly complete. The weak cross sections for ^{208}Pb(p,p') (Table IV) yield admixtures of $d_{5/2}f_{5/2}$, $d_{5/2}p_{3/2}$, and $g_{9/2}f_{7/2}$ of about 20%, 2%, and below 30%, respectively, in congruence with the finding of a dominant $h_{9/2}d_{5/2}$ component in the 5675 state.

The 5492 4^- state with dominant configuration $d_{5/2}f_{5/2}$ and the 5490 6^- state with dominant configuration $h_{9/2}d_{5/2}$. The SSM predicts eight states with the spin of 6^- at $E_x^{\rm SSM} < 6487$ keV [13]. The composition of the four lowest states had been determined in 1981 (now slightly updated [31]); the next two states are rather pure [15]. The highest state below $E_x < 5.85$ MeV with order number $M = 8$ contains 90% $g_{7/2}f_{7/2}$ strength and 10% $h_{9/2}d_{5/2}$ strength [17].

The only missing configuration is the complement of the 5686 6^-_8 state. It is predicted to have 10% $g_{7/2}f_{7/2}$ strength and 90% $h_{9/2}d_{5/2}$ strength. The ^{209}Bi$(d,{}^3$He), ^{209}Bi$(t,\alpha\gamma)$ reactions show the 5.49 MeV level to contain a large $h_{9/2}d_{5/2}$ strength [10–12].

The exclusive excitation on the $g_{9/2}$ IAR assigns the spin of 6^- to the 5490 state; the exclusive excitation on the $d_{5/2}$ IAR the spin of 4^- to the 5492 state (Tables II and IV, Fig. 4).

The 5492 4^-_{10} state contains a major $d_{5/2}f_{5/2}$ component and a strong $h_{9/2}d_{5/2}$ admixture; the 5490 6^-_7 state contains besides a strong $h_{9/2}d_{5/2}$ component about 20%, $g_{9/2}f_{7/2}$ and 0.3% $g_{9/2}p_{3/2}$ strength. Both states (5490 6^-_7 and 5492 4^-_{10}) are weakly excited on the $i_{11/2}$ IAR while only the 5492 4^- state is excited near the $g_{7/2}$, $d_{3/2}$ doublet IAR.

The ^{207}Pb(d,p) cross section for the 5492 4^- state is explained by a 1.5% $g_{7/2}p_{1/2}$ component (Sec. III C). The 5490 6^- state is not excited by the ^{207}Pb(d,p) reaction.

By attributing a considerable fraction of the $h_{9/2}d_{5/2}$ strength observed for the 5.92 MeV level to the 5490 6^- state, the sum rule and normality relations for spins 4^- and 6^- are rather well fulfilled.

The 5648 3^- state with dominant configuration $g_{9/2}f_{7/2}$. The 5649 state contains more than half of the $j_{15/2}p_{3/2}$ strength for the spin of 9^+; the remaining fraction is contained in the 5899 9^+ state [13]. Both states are suggested to share the major strength of the undetectable configuration $i_{11/2}i_{13/2}$ (Sec. IV D 10).

The ^{209}Bi$(t,\alpha\gamma)$ reaction excludes the spin of 2^- for the 5648 state, 60% of the γ intensity is observed to populate two 5^- states [12]. The spin of 4^- is excluded since fourteen 4^- states are identified; they are completely described by the lowest fourteen 4^- particle-hole configurations predicted by the SSM (Table I).

The 5648 is assigned the spin of 3^-. The angular distribution of the 5648 3^- state on the $g_{9/2}$ IAR is described by $40 \pm 20\%$ $g_{9/2}f_{7/2}$ strength (see Fig. 5 in Ref. [17]). A considerable admixture of $d_{5/2}p_{3/2}$ and $d_{5/2}f_{5/2}$ is also observed [13]). The $h_{9/2}d_{5/2}$ strength is determined as about 30% [12].

The 5648 3^- and the 5649 9^+ states have similar mean cross sections on the $d_{5/2}$ and $j_{15/2}$ IAR. The cross section of the 5649 9^+ state near the $d_{5/2}$ IAR is still at 50% of its maximum. Both angular distributions add up incoherently; their shapes are similar.

The 5643 2^- state with dominant configuration $d_{5/2}f_{5/2}$. According to NDS2007, the doublet at $E_x = 5.64$ MeV contains five states: the 5640 1^-, 5642 2^+ states, and the 5643 state with unknown spin; the 5648 3^-, 5649 9^+ states are discussed in the previous paragraph.

The 5640, 5643 states are assigned the spins of 1^-, 2^-, respectively. The ^{208}Pb$(n,n'\gamma)$ reaction shows the 5640 and 5642 states to deexcite to the ground state.

The SSM predicts ten states with the spin of 2^- at $E_x^{\rm SSM} < 6487$ keV [13]. The composition of the yrast state was determined in 1973 [29]. The next two states ($M = 2,3$) share the $d_{5/2}p_{1/2}$ strength and the undetectable $f_{7/2}d_{3/2}$ strength; little other admixtures are present (Fig. 1, Table I). The 5548 2^- state ($M = 4$) contains a large $d_{5/2}f_{5/2}$ component. The states with order numbers $M = 6$–10 contain the complete $d_{5/2}p_{3/2}$ strength [20], about half of the $s_{1/2}p_{3/2}$ and much $s_{1/2}f_{5/2}$ strength [18], and some $d_{3/2}f_{5/2}$ strength in addition [5].

The 5643 2^- state is strongly excited on the $d_{5/2}$ IAR. The angular distribution indicates a strong $d_{5/2}f_{5/2}$ component with a $d_{5/2}p_{3/2}$ admixture. The excitation on the $g_{9/2}$ IAR is weak.

The 5640 1^- state with dominant configuration $g_{9/2}f_{7/2}$. The ^{207}Pb(d,p) reaction excites the 5640 1^-state, but the 5643 2^- state is barely visible. The energy of the γ transition to the ground state observed by the ^{207}Pb$(d,p\gamma)$ reaction [12] differs from the value obtained by the ^{208}Pb$(n,n'\gamma)$ reaction [14]; the energy and its uncertainty agree, however, with the centroid energy of the 5640 1^-, 5643 2^- states determined by the $(p,p'\gamma)$ reaction via IAR in ^{209}Bi [6,40] (Sec. III C). All three states of the 5640 1^-, 5642 2^+, 5643 2^- doublet may contribute to the ground state γ transition.

The 5640 1^- state is mainly excited on the $g_{9/2}$ IAR. A state with dominant $g_{9/2}f_{7/2}$ strength and spin 1^- has an angular distribution strongly peaked towards scattering angles $\Theta = 0^\circ$ and 180° [Fig. 2(a)]; the cross section at $|\Theta - 90^\circ| < 30^\circ$ is suppressed by about 50% in relation to the mean cross section. Data taken on the $g_{9/2}$ IAR are available for $48^\circ \leqslant \Theta \leqslant 115^\circ$. In this view, the angular distribution can be interpreted by a strong $g_{9/2}f_{7/2}$ component. The weak ^{207}Pb(d,p) cross section is explained by a $s_{1/2}p_{1/2}$ component; the weak excitation on the $s_{1/2}$ IAR corroborates it [22]. The weak excitation on the $g_{7/2}$ IAR (Fig. 9) may by explained by a small $g_{7/2}f_{5/2}$ admixture.

The 5640 1^- state is observed in the $(p,p'\gamma)$ reaction by Cramers *et al.* [6]. In the study of the $(p,p'\gamma)$ reaction via IAR in ^{209}Bi by Radermacher *et al.* [40], the 5640 1^-, 5643 2^- states are not resolved; the uncertainty of the energy is five times larger than in most cases. The given energy of 5641.4 ± 0.5 keV would indicate a ratio 2 : 3 for the excitation of the two states.

The relative γ intensities on the $d_{5/2}$, $s_{1/2}$, $g_{7/2}$+$d_{3/2}$ IARs are 10 : 8 : 0 [40]. The large γ intensity on the $s_{1/2}$ IAR is explained by the $s_{1/2}p_{1/2}$ admixture in the 5640 1^- state observed by the ^{207}Pb(d,p) reaction (Table IV).

The strong γ ray $E_\gamma = 1413$ keV observed by the ^{208}Pb$(n,n'\gamma)$ experiment placed as transition from the 4611 8^+ state to the 3198 5^- state partially explains the transition from the 5675 4^- state to the 4262 4^- state [14]. A third placement could explain the depopulation of the 5643 2^- state by the transitions $p_{3/2} \to p_{1/2}$ to the 4230 2^- state with the spectator $d_{5/2}$, and $f_{7/2} \to f_{5/2}$ with the spectator $g_{9/2}$. The $E2$ transition should yield a stronger γ intensity than the $E3$ transition $4611 \to 3198$.

The close energies for the three transitions may explain the missing identification of the 5643 2^- state by the ^{208}Pb$(n,n'\gamma)$ experiment. [Several more additional placements of γ rays both from the ^{209}Bi$(t,\alpha\gamma)$ and ^{208}Pb$(n,n'\gamma)$ reactions are found which may explain the transition from the 5643 2^- state to lower states by the exchange of a single valence nucleon.]

The 5214 5^- state with dominant configuration $f_{7/2}d_{3/2}$. The SSM predicts twelve states with the spin of 5^- at $E_x^{\rm SSM} < 6361$ keV [13]. The composition of the six lowest states was determined in 1973 [29], now updated [31]; the next two states are rather pure [15]. The highest state below $E_x < 5.7$ MeV ($M = 12$) contains about 60% $g_{7/2}f_{7/2}$ strength [17], the 5545 state with order number $M = 11$ much $h_{9/2}d_{5/2}$ strength [10,12]. The spin of the 5482 state ($M = 10$) is determined as 5^- [14]; the ^{208}Pb(p,p') data indicates a strong $d_{5/2}f_{5/2}$ component.

The only missing configuration is the proton configuration $f_{7/2}d_{3/2}$ with the spin of 5^-. The strong configuration mixing among the natural parity configurations, however, suggests a considerable admixture of neutron particle-hole configurations which can be determined by ^{208}Pb(p,p') via IAR.

The 5213 6^+ state is resonantly excited on the $j_{15/2}$ IAR, the 5214 5^- state on the $d_{5/2}$ IAR [13] and clearly on the $g_{9/2}$ IAR (Fig. 4). The distance between the two states is about 0.8 ± 0.6 keV, in rough agreement with 1.91 ± 0.04 keV [14].

The cross section on the $d_{5/2}$ IAR corresponds to about 20% $d_{5/2}f_{5/2}$ strength in the 5214 5^- state; the deep minimum of the angular distribution at $\Theta = 90^\circ$ (the steep raise at $\Theta \lesssim 50^\circ$) agrees with the predicted shape [Fig. 2(a)]. The mean cross section on the $g_{9/2}$ IAR is enhanced in relation to that on the following $i_{11/2}$ IAR. An admixture of about 20% $g_{9/2}f_{7/2}$ strength for the spin of 5^- explains it; a weak $g_{9/2}p_{3/2}$ component with less than 2% strength may be also present.

The ^{207}Pb(d,p) angular distribution of the 5214 5^- state can be interpreted by a 0.03% $g_{9/2}p_{1/2}$ component instead of a 0.05% $d_{5/2}p_{1/2}$ as done by Valnion [32] (Sec. III C). The angular distribution of the analyzing power restricts the $i_{11/2}p_{1/2}$ strength to less than 0.1%.

NDS2007 suggests the doublet at $E_x = 5.21$ MeV to contain a 5^- state besides the 5213 6^+, 5216 4^+ states. The spin of 5^- is thus confirmed and a dominant (undetectable) proton configuration $f_{7/2}d_{3/2}$ derived.

The 4937 3^- state with dominant configuration $i_{11/2}f_{5/2}$. The 4937 state is weakly excited on the $d_{5/2}$ IAR. The angular distribution with polarized deuterons indicates the presence of both $d_{3/2}p_{1/2}$ and $d_{5/2}p_{1/2}$ [32] (Sec. III D). The spin assignment by NDS2007 is accepted. In contrast to the higher spins [15], for the spin of 3^- the configuration $i_{11/2}f_{5/2}$ is in fact undetectable, the direct-(p,p') contribution is rather large (Sec. IV D 1).

The 5195 3^- state with dominant configuration $f_{7/2}s_{1/2}$. NDS2007 suggests the 5.195 MeV doublet to contain besides the 5194 5^+, 5196 7^+ states a third state with negative parity. Indeed, the ^{207}Pb(d,p) reaction excites the 5.195 MeV level. The value of the orbital angular momentum $L \neq 7$ confirms a negative parity state besides the 5196 7^+ state to be excited (Sec. III C). No clear resonance effect is seen with the ^{208}Pb(p,p') reaction.

The 5195 state is assigned the spin of 3^- as suggested by NDS2007; the spin of 4^- is excluded. Namely, the strength of the lowest fourteen 4^- configurations predicted by the SSM below $E_x = 6.3$ MeV (including the undetectable proton configurations $f_{7/2}s_{1/2}$, $f_{7/2}d_{3/2}$) is completely located in the lowest fourteen 4^- states (Table I).

The angular distribution measured with polarized deuterons is interpreted by a 1% $g_{7/2}p_{1/2}$ strength [32]; the angular distribution of the analyzing power clearly yields $J = L - 1/2$. The corresponding ^{208}Pb(p,p') data taken on the $g_{7/2}$ IAR are imprecise, but upper limits of 3% strength for $g_{7/2}p_{1/2}$, $g_{7/2}p_{3/2}$ admixtures are derived.

The matching of the 5195 3^- state with the $f_{7/2}s_{1/2}$ configuration is rather arbitrary as explained in Sec. IV D 1.

The 4953 3^+ state with dominant configuration $g_{9/2}i_{13/2}$. The 4953 state is assigned the spin of 3^- by NDS2007 based on the fit of the angular distribution for the ^{208}Pb(p,p') reaction at $E_p = 35$ MeV with $L = 3$ [45] and the γ transition to the 2615 3^- state in the ^{208}Pb$(n,n'\gamma)$ reaction.

The 4953 state is assigned positive parity in contrast to the assignment by NDS2007. Without any exception, all seventeen 3^- states at $E_x < 6.2$ MeV are excited by the ^{207}Pb(d,p) reaction; the 4953 state, however, is not excited. The mean cross section for the ^{208}Pb(p,p') reaction [Eq. (13)] is less than about 2 μb/sr at all proton energies $E_p = 14.8$–18.2 MeV. On the $g_{9/2}$ IAR, the cross section equals the expected value for the configuration $g_{9/2}\, i_{13/2}$ (Tables II and IV).

The chaos theory predicts a level repulsion between any states of the same spin and parity, in effect yielding a minimal distance. It may confirm the parity assignment to the 4953 state.

The minimal distance observed between any two states of the same spin and parity at $E_x < 6.1$ MeV is 34–37 keV, namely 34 keV between the 5778 and 5812 2^- states and 37 keV between the 4937 and 4974 3^- states (Table I). The distance of the 4953 state to the neighboring 3^- states, $\tilde{E}_x =$ 4937,4974 with 16 and 21 keV, is much less than the observed minimal distance.

The 5235 11^+ state with dominant configuration $g_{9/2}i_{13/2}$ has been identified by deep inelastic scattering with heavy ions (energies of 5.7–6.5 MeV/nucleon) [50]. The ^{208}Pb(p,p') data are in agreement with a strong $g_{9/2}i_{13/2}$ component and an admixture of less than 10% $j_{15/2}f_{7/2}$ (Sec. III D, Tables II and IV).

The 5383 4^+ state with a dominant multi-particle-hole configuration. The 5383, 5385 doublet is well resolved in spectra taken near the $i_{11/2}$ and $j_{15/2}$ IARs although the ratio of the cross sections is larger than 10; the distance between the two states is only 1.8 keV (Tables III and IV). The weaker state on the lower energy side is resolved by the asymmetric peak shape [13] (Fig. 3).

The 5383 state does not exhibit any resonance behaviour, but is weakly excited by the ^{208}Pb(p,p') at all proton energies (Table I). The two lowest 3^+ and the three lowest 5^+ states predicted by the SSM are identified (4953 3^+ [see above], 5262 3^+, and 4929 5^+, 5193 5^+, 5588 5^+ [13]). The SSM predicts the next 3^+ and 5^+ states at $E_x^{\rm SSM} = 5843$ keV with the configuration $i_{11/2}i_{13/2}$. States with more particle-hole configurations and unnatural parity are not expected at such a low excitation energy, hence the 5383 state is assigned the spin of 4^+.

D. Locating the dominant particle-hole configuration strength

1. Configuration mixing in states with the spin of 3^-

The strongest configuration mixing among states below $E_x = 6.4$ MeV is observed for the states with the spin of 3^-. Although the number of configurations for spins 2^- and 3^- below $E_x^{\rm SSM} = 6536$ keV is almost the same (13 and 16), the configuration mixing among the 2^- configurations is much less. Here, more than 90% of the total strength is contained in two states (Fig. 1).

In contrast, in each 3^- state three or more configurations are needed to complement the normality relation to more than 90% [Eq. (6)]; see Table I. There are only six out of seventeen 3^- states where the leading configuration is detected with about 50% strength, namely the 4698, 4974, 5648, 5813, 5874, 6011 states. For all other states the leading strength may be either around 50% with a large uncertainty or it is lower than 50%.

In addition, many 3^- states are strongly excited by the direct-(p,p') reaction at forward scattering angles. For this reason, the strength of the leading configurations in 3^- states can be determined only roughly. Hence, matching each state with a certain SSM configuration is often arbitrary. Yet a one-to-one correspondence can be established.

2. Limited number of configurations in each state

In the following, information about the strength of particle-hole configurations in negative parity states is given. We do not discuss the configuration strengths in positive parity states; see, however, Sec. IV C and the study of states with dominant configurations $j_{15/2}lj$, $lj = p_{1/2}$, $p_{3/2}$, $f_{5/2}$ [13] and $h_{9/2}h_{11/2}$ [10–12].

Except for the spin of 3^-, mostly less than four configurations have to be considered, often even only two configurations contain more than 90% of the total strength. In fact, the transformation matrices [Eqs. (1), (4), and (5)] of all states at $E_x < 6.1$ MeV for spins from 0^- to 8^- are well described by banded matrices with less than two diagonals besides the central diagonal [$B^{I^\pi} = 1$ or 2, Eq. (8)]

Note that for the spins of 1^- and 3^-, the yrast state shows up in addition to the predictions by the SSM for configurations below $E_x = 6.3$ MeV. Hence here the diagonal in the banded matrices is shifted to $M = m + 1$; see Table I and the following paragraph.

3. The 1^- and 3^- yrast states

The 2615 3^- state was detected by the ^{207}Pb(d,p) and the ^{209}Bi$(d,{}^3$He) reactions with low spectroscopic factors [10,36]. The excitation by the ^{208}Pb(p,p') reaction via IAR in ^{209}Bi reveals a remarkable interference pattern for $14 < E_p < 20$ MeV [1,4]. The measurement at one scattering angle only does not allow a quantitative analysis. Yet clearly the amplitude of any particle-hole configuration is weak. No configuration is dominantly excited. Early calculations suggest the 2615 3^- state to contain no strength larger than a few percent [51].

The ^{207}Pb(d,p) reaction shows no detectable configuration in the 4841 1^- state to have a strength larger than a few percent. The ^{208}Pb(p,p') reaction via IAR shows an expressive interference pattern for $14 < E_p < 18$ MeV. No dominant particle-hole configuration can be determined.

4. The $LJ\,p_{1/2}$ strength for $LJ = s_{1/2}, d_{3/2}, d_{5/2}, g_{7/2}, g_{9/2}, i_{11/2}$

In the following, the sum rules $S^{I^\pi}_{LJlj}$ [Eq. (9)] and the spin weighted sum of the strength S_{LJlj} (Eq. (10), Table I) are investigated.

The $LJ\,p_{1/2}$ strength ($LJ = s_{1/2}$, $d_{3/2}$, $d_{5/2}$, $g_{7/2}$, $g_{9/2}$, $i_{11/2}$) was determined by the ^{207}Pb(d,p) reaction with the multigap magnetic spectrograph at Heidelberg [36] and with polarized deuterons at the Q3D magnetic spectrograph at MLL (Garching) [32]. Weak admixtures down to 0.1% strength are determined by recent experiments with the Q3D magnetic spectrograph and unpolarized deuterons [15].

The sum rule $S^{I^\pi}_{LJlj}$ [Eq. (9)] is fulfilled within 5%–20% in most cases, although only two states are considered (Table I):

(i) the main $g_{9/2}p_{1/2}$ strength is located in the 3475 4^-, 3198 5^-, 3708 5^- states [31,36] yielding $S_{LJlj} = 0.86$;
(ii) the main $i_{11/2}p_{1/2}$ strength is located in the 4125 5^-, 4180 5^-, 4206 6^- states [31,32] yielding $S_{LJlj} = 0.84$;
(iii) the main $d_{5/2}p_{1/2}$ strength is located in the 4230 2^-, 5038 2^-, 5127 2^-, 4698 3^-, 4974 3^-, 5245 3^- states [20,32] yielding $S_{LJlj} = 0.78$;
(iv) the main $s_{1/2}p_{1/2}$ strength is located in the 5280 0^-, 5599 0^-, 5292 1^-, 5512 1^- states [18,32] yielding $S_{LJlj} = 0.92$;
(v) the main $g_{7/2}p_{1/2}$ strength is located in the 5874 3^-, 6011 3^-, 5969 4^- states [32] yielding $S_{LJlj} = 0.86$;
(vi) the main $d_{3/2}p_{1/2}$ strength is located in the 5512 1^-, 5947 1^-, 5924 2^-, 6087 2^- states [32] yielding $S_{LJlj} = 0.94$.

5. The $LJ\,p_{3/2}$ strength for $LJ = s_{1/2}, d_{5/2}, g_{9/2}, i_{11/2}$

The $LJ\,p_{3/2}$ strength ($LJ = s_{1/2}$, $d_{5/2}$, $g_{9/2}$, $i_{11/2}$, $j_{15/2}$) is determined by the ^{208}Pb(p,p') reaction via IAR in ^{209}Bi [9,13,15–20]. The sum rule $S^{I^\pi}_{LJlj}$ [Eq. (9)] is fulfilled within 10% in most cases:

(i) the main $g_{9/2}p_{3/2}$ strength is located in the 4051 3^-, 4698 3^-, 4262 4^-, 4359 4^-, 4180 5^-, 4297 5^-, 4383 6^-, 4481 6^- states [29,31] yielding $S_{LJlj} = 0.84$;
(ii) the main $i_{11/2}p_{3/2}$ strength is located in the 5239 4^-, 5276 4^-, 5075 5^-, 5080 6^-, 5085 6^- states [15] yielding $S_{LJlj} = 0.96$;
(iii) the main $d_{5/2}p_{3/2}$ strength is located in the 6264 1^-, 6314 1^-, 5778 2^-, 5812 2^-, 5813 3^-, 5874 3^-, 5886 3^-, 6012 4^- states [20] yielding $S_{LJlj} = 0.90$;
(iv) the main $s_{1/2}p_{3/2}$ strength is located in the 6314 1^-, 6420 2^-, 6552 2^- states [18], but about half of the strength is still not yet identified (and expected at higher excitation energies), $S_{LJlj} = 0.54$;
(v) the main $g_{7/2}p_{3/2}$, $d_{3/2}p_{3/2}$ strength is observed at $6.5 < E_x < 7.5$ MeV [5,9] but not yet identified.

6. The $g_{9/2}f_{7/2}$ strength

The $g_{9/2}f_{7/2}$ strength is determined by the ^{208}Pb(p,p') reaction via IAR in ^{209}Bi [17]. It is mainly located in the 5640 1^- (Sec. IV C), 5778 2^-, 5812 2^-, 5517 3^-, 5648 3^- (Sec. IV C), 5886 4^-, 5214 5^-, 5545 5^-, 5659 5^-, 5490 6^- (Sec. IV C), 5686 6^-, 5543 7^-, 5694 7^-, 5836 8^- states [17,20]. The sum rule $S^{I^\pi}_{LJlj}$ [Eq. (9)] is fulfilled for spins 6^-, 7^-, 8^- and by more than 50% for spins 1^-–5^-. The spin weighted sum rule yields $S_{LJlj} = 0.92$.

7. The $LJ\,f_{5/2}$ strength for $LJ = s_{1/2}, d_{5/2}, g_{9/2}, i_{11/2}$

The $LJ\,f_{5/2}$ strength ($LJ = s_{1/2}$, $d_{5/2}$, $g_{9/2}$, $i_{11/2}$, $j_{15/2}$) is determined by the ^{208}Pb(p,p') reaction via IAR in ^{209}Bi [9,13,15–20]. Despite the larger uncertainty, the sum rule $S^{I^\pi}_{LJlj}$ [Eq. (9)] is fulfilled within 5%–30% in most cases:

(i) the main $g_{9/2}f_{5/2}$ strength is located in the 4230 2^-, 4051 3^-, 4255 3^-, 3995 4^-, 3708 5^-, 3961 5^-, 3920

6^-, 4383 6^-, 4037 7^- states [29,31] yielding $S_{LJlj} = 0.86$;

(ii) the main $i_{11/2}f_{5/2}$ strength is located in the 4937 3^-, 4712 4^-, 4709 5^-, 4762 6^-, 4680 7^-, 4919 8^- states [15] yielding $S_{LJlj} = 0.92$;

(iii) the main $d_{5/2}f_{5/2}$ strength is located in the 5280 0^-, 5599 0^-, 5292 1^-, 5512 1^-, 5548 2^-, 5643 2^-, 5347 3^-, 5648 3^-, 5492 4^-, 5675 4^-, 5482 5^-, 5659 5^- states (Sec. IV C) yielding $S_{LJlj} = 0.76$.

The $s_{1/2}f_{5/2}$ strength can be determined only with difficulty in the presence of major $d_{5/2}p_{3/2}$ components. The interference between the two components changes the shape of the angular distribution: it is no longer isotropic; namely the distance between the $d_{5/2}$ and $s_{1/2}$ IARs is only about twice the width of each IAR [5]. The deviation from isotropy is already observed for the states with strong $s_{1/2}p_{3/2}$ components and little $d_{5/2}p_{3/2}$, $d_{5/2}f_{5/2}$ admixtures [18].

8. The $h_{9/2}lj$ strength for $lj = s_{1/2}, d_{3/2}, d_{5/2}$

The $h_{9/2}lj$ strength ($lj = s_{1/2}, d_{3/2}, d_{5/2}$) was determined by the ^{209}Bi(d,^{3}He) reaction [10]. The sum rules for the configurations $h_{9/2}s_{1/2}$, $h_{9/2}d_{3/2}$ were discussed by Grabmayr *et al.* [10] and by Schramm *et al.* [12], for the configuration $h_{9/2}d_{5/2}$; see Secs. IV A and IV C:

(i) the main $h_{9/2}s_{1/2}$ strength is located in the 3947 4^-, 4262 4^-, 3708 5^-, 3961 5^- states [10,31] yielding $S_{LJlj} = 0.86$;

(ii) the main $h_{9/2}d_{3/2}$ strength is located in the 4051 3^-, 4698 3^-, 4262 4^-, 4359 4^-, 4125 5^-, 4180 5^-, 4383 6^-, 4481 6^- states [10,29,31] yielding $S_{LJlj} = 0.82$;

(iii) the main $h_{9/2}d_{5/2}$ strength is located in the 5548 2^- 5778 2^-, 5385 3^-, 5648 3^-, 5492 4^-, 5675 4^-, 5545 5^-, 5659 5^-, 5490 6^-, 5686 6^-, 5543 7^-, 5694 7^- states yielding $S_{LJlj} = 0.88$.

9. The $f_{7/2}s_{1/2}$, $f_{7/2}d_{3/2}$ strength

The $f_{7/2}s_{1/2}$, $f_{7/2}d_{3/2}$ strength is not detectable by any experiment; a target of ^{209}Bi prepared in the first excited state cannot be produced.

The determination of some $f_{7/2}s_{1/2}$, $f_{7/2}d_{3/2}$ strength relies on the assumption that an ensemble including the neighboring states may be described by a unitary transformation of an equivalent number of configurations. If the amplitudes $c_{LJ,lj}^{\tilde{E}_x I^\pi}$ of all states for each configuration but one can be determined [Eqs. (1), (4), and (5)] then the amplitudes of the undetectable configuration is derivable.

All states with spins 2^-–5^- predicted by the SSM below $E_x = 6.3$ MeV are identified at $E_x < 6.1$ MeV and most of their configuration strengths are determined (Table I). Hence the orthogonality relations [Eqs. (6) and (7)] may be used to deduce the strength of undetectable configurations.

For the spin of 3^-, the strengths of the undetectable configurations $f_{7/2}s_{1/2}$, $f_{7/2}d_{3/2}$, and $i_{11/2}f_{5/2}$ which is also in fact also undetectable, are discussed in Sec. IV D 1. For the spins 2^-, 4^-, 5^- see Secs. IV A and IV C.

Although the configurations $f_{7/2}s_{1/2}$, $f_{7/2}d_{3/2}$ are undetectable, the spin weighted sum rule S_{LJlj} [Eq. (10)] yields $S_{f_{7/2}s_{1/2}} = 0.81$, $S_{f_{7/2}d_{3/2}} = 0.73$ (Table I).

10. The $g_{9/2}i_{13/2}$, $i_{11/2}i_{13/2}$, $j_{15/2}i_{13/2}$ strengths

Because of the low penetrability, the neutron particle-hole configurations $g_{9/2}i_{13/2}$, $i_{11/2}i_{13/2}$, $j_{15/2}i_{13/2}$ exhibit a measurable resonance effect in the presence of the direct-(p,p') reaction only in rare cases. Yet in this paper, the lowest 3^+ state with the dominant $g_{9/2}i_{13/2}$ strength is identified at $E_x = 4953$ keV, and the 5235 11^+ state with the dominant $g_{9/2}i_{13/2}$ strength is confirmed (Sec. IV C).

Admixtures of the configuration $j_{15/2}i_{13/2}$ are effectively not detectable by experiment. In addition, the SSM predicts the configurations $g_{7/2}f_{5/2}$, $d_{3/2}f_{5/2}$ to have similar excitation energies (Table I). Therefore the 3–6 states with spins from 1^- to 6^- predicted by the SSM in the region $E_x \approx 6.4$ MeV (in total about 24 states) are expected to be strongly mixed.

Data obtained by experiments with semiconductor detectors are not yet fully evaluated [9]. Excitation functions were taken by Wharton *et al.* at two scattering angles only [5]. Data for the ^{208}Pb(p,p') reaction on the $g_{7/2}$ and $d_{3/2}$ IARs obtained by the experiments with the Q3D magnetic spectrograph reveal about twenty states with negative parity at $6.2 < E_x < 6.4$ MeV. (Figure 10 shows some of these states.) Except for the 6264 1^- and 6275 3^- states, no other negative parity state is identified [14].

E. Mixing among configurations with unnatural and natural parity

1. Determination of the configuration mixing

A fit of the lowest twenty negative parity states was done in 1973 [29]. The main experimental data derived from the work of H.-J. Glöckner [9]; spectroscopic information about the proton particle-hole configurations from Refs. [47,49] was used. In 1981 new experiments with ^{209}Bi(d,^{3}He) reaction were performed [10], and an update of the fit was done [31], now with spin assignments proved to be correct [14]. The two largest fragments of each particle-hole configuration in twenty states at $E_x \lesssim 4.5$ MeV are shown in Table I.

As a result from the analysis of the twenty lowest negative parity states [29,31] and the study of positive parity states [13], the configuration mixing in the unnatural parity states is much less than in states with natural parity. The mean value of off-diagonal matrix elements for the residual interaction among the unnatural parity configurations is about 50 keV while it is three times larger for natural parity configurations.

In the meantime, all 70 negative parity states predicted by the SSM below $E_x = 6.3$ MeV are identified (Table I). In the following, we discuss the influence of the nature of parity $(-1)^{L+l+I}$ on the mixing among configurations $LJ\,lj$.

2. Order of configurations and states

As Table I shows, the order number m of the dominant configuration corresponds to the order number M of the states with few exceptions. The striking exceptions are the states with the spins of 1^- and 3^-. Here, the yrast state has no large fraction of any SSM configurations predicted below $E_x = 6.3$ MeV (Sec. IV D 3), and the order number of the dominant SSM configuration in the following states is mostly $M = m + 1$ up to $M = 9$ and 17, respectively. The dominant configuration in the states at $E_x \approx 6.3$ MeV (see Fig. 10) is difficult to determine for spins 1^-, 2^-, 3^-; states with spins 4^-–6^- are not yet identified, but certainly present; see Fig. 10.

The order number of the dominant configuration equals the order number of the state for the spin of 0^- (2 states up to $E_x = 5.6$ MeV), 2^- (10 states up to $E_x = 6.5$ MeV), 6^- (8 states up to $E_x = 5.9$ MeV), 7^- (5 states up to $E_x = 5.7$ MeV), and 8^- (2 states up to $E_x = 5.9$ MeV).

The same is true for the spin of 4^- (13 states up to $E_x = 6.1$ MeV) except for the reversal of $m, M = 8{,}9$ and $13{,}14$. The SDI extension of the SSM [21] explains the reversals by the contrary shift of the two pairs of configurations; the predicted excitation energies are 5143, 5291 and 6002, 6022 keV while the SSM predicts energies are 5162, 5108 and 5922, 5896 keV, respectively.

For the natural parity states with spins 1^- (9 states up to $E_x = 6.4$ MeV), 3^- (17 states up to $E_x = 6.2$ MeV), and 5^- (12 states up to $E_x = 5.7$ MeV) several reversals of the order numbers m, M show up. For the spin of 5^- the declaration of a dominant configuration in the states with order number $M = 2$–6 is difficult; for the spin of 3^- see Sec. IV D 1. In addition the order number M is shifted by $+1$ for spins 1^- and 3^- because of the yrast state (Sec. IV D 3).

These facts show that the residual interaction among natural parity particle-hole configurations is much larger than among unnatural parity configurations. For the spin of 7^- the separation between the configurations is much wider, hence the configuration mixing is low.

3. Strength of the configuration mixing

Among the 6^- states, the states with order number $M = 1$, 2, 5, 6, 7, 8 contain 90% of the corresponding configuration, the $M = 3{,}4$ pair shares almost the full strength of the configurations $m = 3{,}4$.

Most 4^- states consist by more than 95% of one or two configurations with less than a few percent strength of other configurations. The 4^- states with order number $M = 1$, 2, 3, 6, 7, 8, 9 contain more than 90% of the corresponding configuration with order number $M = m$, the 4^-_{13} state 90% of the 14th configuration. The $M = 4{,}5$ pair contains litte admixtures from other configurations but $m = 4{,}5$. The ensemble of 4^- states with order numbers $M = 12$, 13, 14 consists almost entirely of the corresponding configurations.

Among the 2^- states, the yrast state contains 90% of the corresponding configuration, and the following states build pairs which share almost the full strength of the corresponding configurations, $M = 2{,}3$, $M = 4{,}5$, $M = 6{,}7$, and $M = 8{,}9$; see Fig. 1. Only the states beginning with $M = 10$ are more strongly mixed and contain unknown fractions of the following configurations [18].

Admixtures of all detectable configurations ($i_{11/2}f_{5/2}$, $i_{11/2}f_{7/2}$, $g_{9/2}f_{7/2}$, $g_{9/2}h_{9/2}$) in the two 8^- states are less than a few percent, thus 98% strength is a reasonable estimate for the $i_{11/2}f_{5/2}$, $g_{9/2}f_{7/2}$ configurations, respectively.

Because of the large spacing between the SSM configurations, most 7^- states contain more than 90% of the corresponding configuration. Similarly, except for the yrast state, the 1^- states at $E_x < 6.1$ MeV are less mixed than the 2^-, 3^-, 5^- states since the mean distance between the SSM configurations is about 150 keV.

In contrast, the 5^- states are much more mixed than the 4^- states although the number of configurations differs only slightly; the SSM predicts fourteen 4^- configurations and twelve 5^- configurations below 6 MeV. Except for the $M = 7{,}8$ states, no state contains more than 70% strength. Especially, the yrast 5^- state contains besides 70% strength of the corresponding SSM configuration, $g_{9/2}p_{1/2}$, at least five other configurations with similar strengths; the second 5^- state is even more mixed [31].

The strongest configuration mixing is determined for the 3^- states (Sec. IV D 1). No state contains more than 70% of any single configuration. The number of SSM configurations with either spin 0^-–14^-, 1^+–12^+ below $E_x \approx 7.2$ MeV is the highest for the spin of 3^-; only for the spin 4^- is a similar number of configurations at $E_x < 7.4$ MeV predicted, namely 23 instead of 24. Yet, the difference in the configuration mixing is striking. Each 3^- state has at least three admixing configurations with a strength larger than 10% while most 4^- states are rather pure.

In summary, the configuration mixing among the states with spin 2^-, 4^-, 6^- is much less than among the states with spin 1^-, 3^-, 5^-. Yet, the number of configurations for spin 2^-–5^- is similar.

F. Centroid energies

The centroid energy $E_x^{\rm cnt}$ for each spin and each configuration $LJ\,lj$ [Eq. (18)] is shown in column 2 of Table I. The difference $E_x^{\rm cnt} - E_x^{\rm SSM}$ to the SSM energy is often close to the value $\delta E_x^{\rm SDI}$ [Eq. (11)] calculated by the SDI [21]. We do not discuss the values here since only one or two states sharing a certain configuration are considered; especially for natural parity states the strength of a certain configuration is often distributed across more states.

The global centroid energy $\overline{E_x^{\rm cnt}}$ [Eq. (19)] differs from the SSM energy for the neutron particle-hole configurations below $E_x = 6361$ keV ($s_{1/2}p_{3/2}$) by less than 10–30 keV if the configuration strengths for all spins are determined by more than 80%.

The nonlinear increase of the Coulomb energy with the atomic weight is assumed as $\Delta E_C = -0.300$ MeV [13]. It is indeed observed as

$$\overline{E_x^{\rm cnt}} - E_x^{\rm SSM} + \Delta E_C = -0.30, -0.27, -0.29\ \text{MeV} \quad \text{for} \quad h_{9/2}\,lj, \quad lj = s_{1/2}, d_{3/2}, d_{5/2}, \tag{22}$$

respectively (Table I). It is smaller for the undetectable proton configurations $f_{7/2}lj$,

$$\overline{E_x^{\text{cnt}}} - E_x^{\text{SSM}} + \Delta E_C = -0.08, -0.24 \text{ MeV for } f_{7/2}s_{1/2},\ f_{7/2}d_{3/2}. \quad (23)$$

The deviations of the centroid energy $\overline{E_x^{\text{cnt}}}(LJ,lj)$ [Eq. (19)] from the predicted SSM energy are especially large for the configurations $s_{1/2}p_{1/2}$, $s_{1/2}f_{5/2}$ (0.13 and 0.21 MeV). Yet the uncertainties of the configuration strengths are large because the angular distributions on the $s_{1/2}$ IAR are not isotropic as expected (Sec. IV D 7).

The 1^- yrare state contains about 80% of the $s_{1/2}p_{1/2}$ strength. The remaining 20% strength is scattered across many states up to 8 MeV [16]. Therefore the difference between the SSM energy and the value E_x^{cnt} is much smaller than indicated (0.12 MeV, see Table I).

V. SUMMARY

NDS2007 and recent publications reveal spins of many negative parity states in ^{208}Pb at $E_x < 7$ MeV. By this work, six new spins are assigned to negative parity states and three new spins to positive parity states, one state has been assigned a new parity; two spins suggested by the NDS2007 are verified. Together with other recent publications, 72 negative parity states below $E_x = 6.1$ MeV are thus identified.

Since 2003, experiments with the Q3D magnetic spectrograph at MLL (Garching, Germany) on the ^{208}Pb(p,p') [and ^{207}Pb(d,p)] reactions were performed. The peak shape is asymmetric with a resolution of about 1.5 keV HWHM on the low excitation energy side. In addition to recent publications, the experiments allow us to disentangle six more doublets with distances less than 2 keV containing 15 states; two doublets have three members within 3 keV.

The configuration mixing among the states with natural parity is stronger than among the states with unnatural parity. For the unnatural parity states with spins 2^- and 4^- one or two states contain more than 90% of a certain configuration, for natural parity states with spins 3^- and 5^- often at least four states are needed to fulfill the sum rule by 80%. The number of configurations at $E_x^{\text{SSM}} \leqslant 6361$ keV, however, is about the same for spins 2^-–5^- (10, 15, 14, 12, respectively.)

In this paper, for clarity, the distribution of each configuration across only one or two states is shown. A one-to-one correspondence between the 70 predicted SSM configurations and 70 states can be established.

The strength of 64 detectable configurations below $E_x = 6.1$ MeV is completely determined by more than 90% in 70 states. Based on the prediction of 70 negative parity configurations by the SSM below $E_x = 6.3$ MeV, the completeness of the sum rules for 64 detectable configurations allows us to assume the sum rules for six undetectable configurations to be nearly complete, too.

The strengths of the undetectable configurations with an $f_{7/2}$ proton particle and spins 2^-–5^- are thus deduced. Most strength of the proton particle-hole configuration $f_{7/2}s_{1/2}$ is located in two states at $E_x = 4911, 5195$ keV and for $f_{7/2}d_{3/2}$ in five states at $5127 \leqslant E_x \leqslant 5276$ keV. Yet no experiment allows us to detect the configurations directly.

As shown for the lowest twenty negative parity configurations [29], a gap in the configuration space larger than the mean residual interaction among different configurations allows us to assume the configuration space below the gap to be rather complete. Indeed, for the spins of 0^-, 4^-, and 5^-–8^- there is a large gap in the space of the predicted configurations, $5568 < E_x^{\text{SSM}} < 6844$, $5922 < E_x^{\text{SSM}} < 6361$, and $5771 < E_x^{\text{SSM}} < 6361$ keV, respectively. The gaps with 1.3, 0.4, and 0.6 MeV are larger than the mean residual interaction of around 100 keV.

For the spins 1^- and 3^-, the gap with less than 200 keV is comparable to the mean residual interaction of about 150 keV. For the spin of 2^- the wide distribution of the $s_{1/2}f_{5/2}$ and $s_{1/2}p_{3/2}$ strengths ($E_x^{\text{SSM}} = 6033$ and 6361 keV) yields no clear gap. However, each 2^- state below $E_x = 6.4$ MeV (excluding the 6420 2^- state) is described by two configurations with together more than 80% strength. Thus a low configuration mixing among the 2^- configurations is indicated, similar to the other unnatural parity states.

An important result is the fact that the 1^- yrast state at $E_x = 4841$ keV and the 3^- yrast state $E_x = 2615$ keV appear in addition. Neither of these yrast states contains any significant admixture of the predicted five and thirteen configurations below $E_x^{\text{SSM}} = 6361$ keV, respectively.

Another result are the Coulomb corrections entering into the calculation of the SSM excitation energies for the proton particle-hole configurations $f_{7/2}s_{1/2}$, $f_{7/2}d_{3/2}$. They are significantly smaller than those derived for the configurations $h_{9/2}s_{1/2}$, $h_{9/2}d_{3/2}$, $h_{9/2}d_{5/2}$, $h_{9/2}h_{11/2}$.

ACKNOWLEDGMENTS

The basic work of M. Martin is highly acknowledged. We thank G. Graw, W. Henning, and R. Krücken for supporting the experiments. We thank F. Riess for much advice on the usage of GASPAN. We thank R. V. Jolos for discussions.

APPENDIX: TABLE OF PUBLISHED SPECTRA

Table V shows references to published spectra for the ^{208}Pb(p,p') reaction. (Survey spectra from Refs. [2,32,52] are included for convenience.) The spectra were taken near the $g_{9/2}$, $i_{11/2}$, $j_{15/2}$, $d_{5/2}$, $s_{1/2}$, $g_{7/2}$, $d_{3/2}$ IARs with resonance energies $E^{\text{res}} = 14.92$, 15.72, 16.39, 16.50, 16.96, 17.43, 17.48 MeV [5] and far off resonance. The entries are ordered by their lowest excitation energies. Most spectra in Refs. [13,15–20] and all spectra in Figs. 3–10 are fitted by GASPAN [38].

The shown spectra are excerpts of 40–400 keV length from about 300 spectra taken with the Q3D magnetic spectrograph at MLL (Garching, Germany) during 2003–2009. The entire length of one spectrum is about 0.9 MeV; it corresponds to a range of about 8% in the momentum of the scattered protons $\sqrt{E_p - E_x^0}$ around a chosen excitation energy E_x^0 where E_p is the bombarding energy.

Table VI shows references to published spectra for the ^{207}Pb(d,p) reaction in the range $4.65 \leqslant E_x \leqslant 6.15$ MeV.

[1] C. F. Moore, L. J. Parish, P. von Brentano, and S. A. A. Zaidi, Phys. Lett. **22**, 616 (1966).
[2] C. F. Moore, J. G. Kulleck, P. von Brentano, and F. Rickey, Phys. Rev. **164**, 1559 (1967).
[3] S. A. A. Zaidi, L. J. Parish, J. G. Kulleck, C. F. Moore, and P. von Brentano, Phys. Rev. **165**, 1312 (1968).
[4] N. Stein, C. A. Whitten, and D. A. Bromley, Phys. Rev. Lett. **20**, 113 (1968).
[5] W. R. Wharton, P. von Brentano, W. K. Dawson, and P. Richard, Phys. Rev. **176**, 1424 (1968).
[6] J. G. Cramer, P. von Brentano, G. W. Phillips, H. Ejiri, S. M. Ferguson, and W. J. Braithwaite, Phys. Rev. Lett. **21**, 297 (1968).
[7] P. Richard, P. von Brentano, H. Wieman, W. Wharton, W. G. Weitkamp, W. W. McDonald, and D. Spalding, Phys. Rev. **183**, 1007 (1969).
[8] J. G. Kulleck, P. Richard, D. Burch, C. F. Moore, W. R. Wharton, and P. von Brentano, Phys. Rev. C **2**, 1491 (1970).
[9] H.-J. Glöckner, Master's thesis, Universität Heidelberg, 1972, edited by A. Heusler, http://www.mpi-hd.mpg.de/personalhomes/hsl/HJG_diplom/ (unpublished); A. Heusler, H.-J. Glöckner, E. Grosse, C. F. Moore, J. Solf, and P. von Brentano (unpublished).
[10] P. Grabmayr, G. Mairle, U. Schmidt-Rohr, G. P. A. Berg, J. Meissburger, P. von Rossen, and J. L. Tain, Nucl. Phys. A **469**, 285 (1987).
[11] P. Grabmayr (private communication). Four spectra of ^{209}Bi(d, ^{3}He) and four spectra of ^{208}Pb(d, ^{3}He) taken with the Big Karl magnetic spectrograph at Jülich in 1981 under similar conditions as [10] are reanalyzed by GASPAN [38] and recalibrated by NDS2007 [14].
[12] M. Schramm, K. H. Maier, M. Rejmund, L. D. Wood, N. Roy, A. Kuhnert, A. Aprahamian, J. Becker, M. Brinkman, D. J. Decman, E. A. Henry, R. Hoff, D. Manatt, L. G. Mann, R. A. Meyer, W. Stoeffl, G. L. Struble, and T.-F. Wang, Phys. Rev. C **56**, 1320 (1997).
[13] A. Heusler, G. Graw, R. Hertenberger, F. Riess, H.-F. Wirth, T. Faestermann, R. Krücken, Th. Behrens, V. Bildstein, K. Eppinger, C. Herlitzius, O. Lepyoshkina, M. Mahgoub, A. Parikh, S. Schwertel, K. Wimmer, N. Pietralla, V. Werner, J. Jolie, D. Mücher, C. Scholl, and P. von Brentano, Phys. Rev. C **82**, 014316 (2010).
[14] M. J. Martin, Nucl. Data Sheets **108**, 1583 (2007).
[15] A. Heusler, G. Graw, R. Hertenberger, F. Riess, H.-F. Wirth, T. Faestermann, R. Krücken, J. Jolie, D. Mücher, N. Pietralla, and P. von Brentano, Phys. Rev. C **74**, 034303 (2006).
[16] A. Heusler, G. Graw, R. Hertenberger, R. Krücken, F. Riess, H.-F. Wirth, and P. von Brentano, Phys. Rev. C **75**, 024312 (2007).
[17] A. Heusler, G. Graw, T. Faestermann, R. Hertenberger, H.-F. Wirth, R. Krücken, C. Scholl, and P. von Brentano, Eur. Phys. J. A **44**, 233 (2010).
[18] A. Heusler, T. Faestermann, R. Hertenberger, R. Krücken, H.-F. Wirth, and P. von Brentano, Eur. Phys. J. A **46**, 17 (2010).
[19] A. Heusler, T. Faestermann, G. Graw, R. Hertenberger, J. Jolie, R. Krücken, D. Mücher, N. Pietralla, C. Scholl, V. Werner, H.-F. Wirth, and P. von Brentano, Eur. Phys. J. A **47**, 22 (2011); **47**, 29(E) (2011).
[20] A. Heusler, T. Faestermann, R. Hertenberger, R. Krücken, H.-F. Wirth, and P. von Brentano, J. Phys. G (London) **38**, 105102 (2011).
[21] A. Heusler, R. V. Jolos, and P. von Brentano, Yad. Fiz. **76**, 860 (2013) [Phys. At. Nuclei **76**, 807 (2013)].
[22] A. Heusler, P. von Brentano, T. Faestermann, G. Graw, R. Hertenberger, J. Jolie, R. Krücken, K. H. Maier, D. Mücher, N. Pietralla, F. Riess, V. Werner, and H.-F. Wirth, in *Proceedings of the 9th International Spring Seminar on Nuclear Physics*, edited by A. Covello (World Scientific, Singapore, 2008), p. 293.
[23] A. Heusler, J. Phys.: Conf. Ser. **267**, 012038 (2011).
[24] A. Heusler, P. von Brentano, T. Faestermann, G. Graw, R. Hertenberger, J. Jolie, R. Krücken, and H.-F. Wirth, J. Phys.: Conf. Ser. **312**, 092030 (2011).
[25] A. Heusler, T. Faestermann, R. Hertenberger, H.-F. Wirth, and P. von Brentano, Eur. Phys. J. Web Conf. **66**, 02049 (2014).
[26] R. Hertenberger, H. Kader, F. Merz, F. J. Eckle, G. Eckle, P. Schiemenz, H. Wessner, and G. Graw, Nucl. Instrum. Methods A **258**, 201 (1987).
[27] M. Löffler, H. J. Scheerer, and H. Vonach, Nucl. Instrum. Methods B **111**, 1 (1973).
[28] H.-F. Wirth, Ph.D. thesis, Technische Universität München, 2001 (unpublished), http://tumb1.biblio.tu-muenchen.de/publ/diss/ph/2001/wirth.html.
[29] A. Heusler and P. von Brentano, Ann. Phys. (NY) **75**, 381 (1973).
[30] J. P. Bondorf, P. von Brentano, and P. Richard, Phys. Lett. B **27**, 5 (1968).
[31] A. Heusler, http://www.mpi-hd.mpg.de/personalhomes/hsl/208Pb_eval/update2013.pdf.
[32] B. D. Valnion, V. Yu. Ponomarev, Y. Eisermann, A. Gollwitzer, R. Hertenberger, A. Metz, P. Schiemenz, and G. Graw, Phys. Rev. C **63**, 024318 (2001); B. D. Valnion, *Leichtionen-induzierte Anregungen in* ^{178}*Hf und* ^{208}*Pb*, Ph.D. thesis, Universität München, 1998 (Herbert Utz Verlag, München, 1998).
[33] L. W. Nordheim, Phys. Rev. **78**, 294 (1950).
[34] A. Heusler, H. L. Harney, and J. P. Wurm, Nucl. Phys. A **135**, 591 (1969).
[35] R. G. Clarkson, P. von Brentano, and H. L. Harney, Nucl. Phys. A **161**, 49 (1971).
[36] P. B. Vold, J. O. Andreassen, J. R. Lien, A. Graue, E. R. Cosman, W. Dünnweber, D. Schmitt, and F. Nüsslin, Nucl. Phys. A **215**, 61 (1973).
[37] D. A. Varshalovich, A. N. Moskalev, and V. K. Khersonskii, *Quantum Theory of Angular Momentum* (World Scientific, Singapore, 1988).
[38] F. Riess, GASPAN, Gamma-ray And particle SPectra interactive and automatic ANalysis, 2006, http://www.it.physik.uni-muenchen.de/dienste/software/gaspan/index.html.
[39] P. E. Garrett (private communication).
[40] E. Radermacher, M. Wilhelm, S. Albers, J. Eberth, N. Nicolay, H. G. Thomas, H. Tiesler, P. von Brentano, R. Schwengner, S. Skoda, G. Winter, and K. H. Maier, Nucl. Phys. A **597**, 408 (1996).
[41] T. Shizuma, T. Hayakawa, H. Ohgaki, H. Toyokawa, T. Komatsubara, N. Kikuzawa, A. Tamii, and H. Nakada, Phys. Rev. C **78**, 061303 (2008).
[42] R. Schwengner, R. Massarczyk, B. A. Brown, R. Beyer, F. Dönau, M. Erhard, E. Grosse, A. R. Junghans, K. Kosev, C. Nair, G. Rusev, K. D. Schilling, and A. Wagner, Phys. Rev. C **81**, 054315 (2010).
[43] A. Tamii, I. Poltoratska, P. von Neumann-Cosel, Y. Fujita, T. Adachi, C. A. Bertulani, J. Carter, M. Dozono, H. Fujita,

K. Fujita, K. Hatanaka, D. Ishikawa, M. Itoh, T. Kawabata, Y. Kalmykov, A. M. Krumbholz, E. Litvinova, H. Matsubara, K. Nakanishi, R. Neveling, H. Okamura, H. J. Ong, B. Özel-Tashenov, V. Yu. Ponomarev, A. Richter, B. Rubio, H. Sakaguchi, Y. Sakemi, Y. Sasamoto, Y. Shimbara, Y. Shimizu, F. D. Smit, T. Suzuki, Y. Tameshige, J. Wambach, R. Yamada, M. Yosoi, and J. Zenihiro, Phys. Rev. Lett. **107**, 062502 (2011).

[44] I. Poltoratska, P. von Neumann-Cosel, A. Tamii, T. Adachi, C. A. Bertulani, J. Carter, M. Dozono, H. Fujita, K. Fujita, Y. Fujita, K. Hatanaka, M. Itoh, T. Kawabata, Y. Kalmykov, A. M. Krumbholz, E. Litvinova, H. Matsubara, K. Nakanishi, R. Neveling, H. Okamura, H. J. Ong, B. Özel-Tashenov, V. Yu. Ponomarev, A. Richter, B. Rubio, H. Sakaguchi, Y. Sakemi, Y. Sasamoto, Y. Shimbara, Y. Shimizu, F. D. Smit, T. Suzuki, Y. Tameshige, J. Wambach, M. Yosoi, and J. Zenihiro, Phys. Rev. C **85**, 041304 (2012).

[45] W. T. Wagner, G. M. Crawley, G. R. Hammerstein, and H. McManus, Phys. Rev. C **12**, 757 (1975).

[46] M. B. Lewis, Nucl. Data Sheets **5**, 243 (1971).

[47] J. H. Bjerregaard, O. Hansen, O. Nathan, R. Chapman, and S. Hinds, Nucl. Phys. A **107**, 241 (1968).

[48] E. A. McClatchie, C. Glashausser, and D. L. Hendrie, Phys. Rev. C **1**, 1828 (1970).

[49] G. Mairle, D. Hartwig, G. Kaschl, H. Mackh, and A. Heusler (private communication).

[50] J. Wrzesinski, K. H. Maier, R. Broda, B. Fornal, W. Królas, T. Pawlat, D. Bazzacco, S. Lunardi, C. Rossi Alvarez, G. de Angelis, A. Gadea, J. Gerl, and M. Rejmund, Eur. Phys. J. A **10**, 259 (2001).

[51] T. T. S. Kuo and G. E. Brown (private communication).

[52] B. D. Valnion, W. Oelmaier, D. Hofer, E. Zanotti-Müller, G. Graw, U. Atzrott, F. Hoyler, and G. Staudt, Z. Phys. A **350**, 11 (1994).